Chapter 3

SULFATE ACCUMULATION IN THE LOS ANGELES SEA BREEZE/LAND BREEZE CIRCULATION SYSTEM

Chapter in Ph.D. Thesis

by

Glen R. Cass
Environmental Quality Laboratory
California Institute of Technology

August 1978

SULFATE ACCUMULATION IN THE LOS ANGELES SEA BREEZE/LAND BREEZE CIRCULATION SYSTEM

Glen R. Cass
Environmental Quality Laboratory
California Institute of Technology
August, 1978

Abstract

An SF_6 tracer study was conducted on July 22, 1977 to examine the origin of the high sulfate concentrations observed in coastal Los Angeles County. It was found that the sea breeze/land breeze circulation system in the Los Angeles Basin results in transport of pollutants seaward at night followed by return of aged material inland the next day. This characteristic wind reversal pattern both increases the retention time for sulfate formation in the marine environment and causes individual air parcels to make multiple passes over large coastal emissions sources. Sulfur oxides recirculated by the previous night's land breeze were found to be the largest single contributor to 24 hour average sulfate air quality on this occasion. In contrast, 24 hour average SO_2 concentrations were dominated by fresh emissions from nearby sources. The overall rate of SO_2 oxidation to form sulfates in the Los Angeles atmosphere was estimated to average about 5.8% per hour during these experiments.

1.0 Introduction

The sea breeze/land breeze circulation system in the Los Angeles Basin results in transport of pollutants seaward at night followed by return of aged material inland the next day. One result of this air mass recirculation pattern is to increase the potential for accumulating high sulfate concentrations. In order to quantify this effect, a sulfate and total sulfur balance was constructed for polluted air masses passing over a coastal air monitoring station in the vicinity of a cluster of major SO_x emission sources.

2.0 Physical Setting

The location of interest is the Santa Monica Bay coastline of Los Angeles County, as shown in Figure 1. The major sources of sulfur oxides emissions in the Los Angeles area are situated at the coast, close to waterborne transportation and a supply of cooling water. One such source grouping shown in Figure 1 is a cluster of two oil-fired power plants and an oil refinery located at El Segundo, California. During 1973, for example, that group of El Segundo point sources accounted for an average of 47.7 short tons per day of SO_x emissions (stated as SO_2). By comparison, sulfur oxides emissions from surrounding low level sources located within a four mile (6.4 km) radius of the El Segundo Power Plant totaled less than 2.7 tons/day.[1]

---

[1] For emissions data, see Cass (1978), Figures 4.15 through 4.20; grid squares I5 through I8 by J11 through J12.

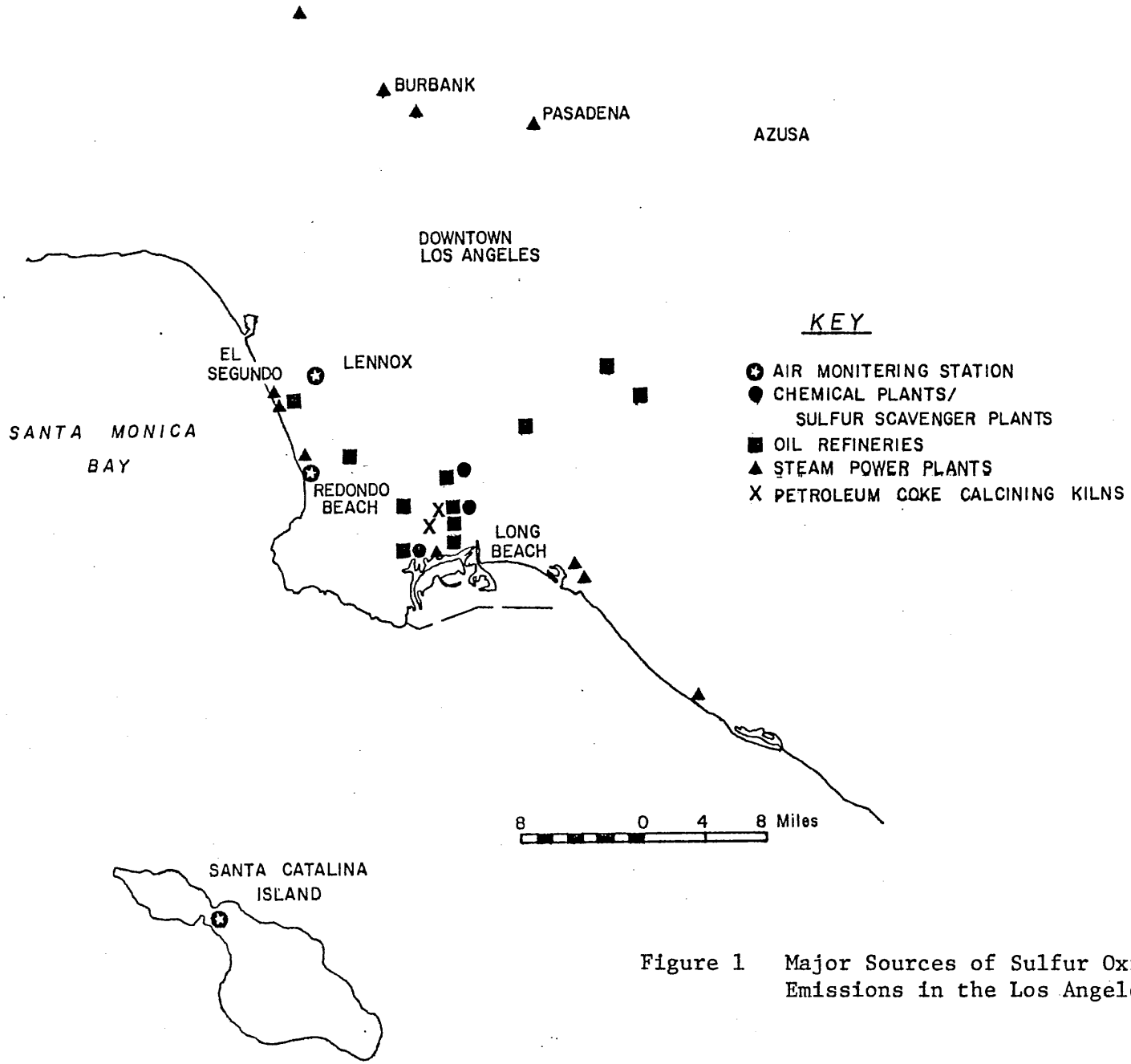

Figure 1 Major Sources of Sulfur Oxides Emissions in the Los Angeles Area

During the daytime, emissions from these coastal sources are advected inland by the sea breeze. In the evening, the onshore winds stagnate and then begin to drain slowly back to sea. Polluted air masses residing over metropolitan Los Angeles during the previous afternoon are swept back toward the coast.

As this "urban backwash" of material previously over land passes the coastline, overnight emissions from elevated sources are injected high into the atmosphere. The urban backwash and overnight coastline emissions are then stored over the Santa Monica Bay during the early morning hours.

Toward sunrise the onset of the sea breeze reestablishes a dominant onshore flow. Aged material stored over the Santa Monica Bay is advected back across the coast, picks up a fresh pollutant burden as it recrosses the coastline emissions sources and proceeds inland. Thus the typical day's sulfate air quality observations made at a near-coastal community might well reflect contributions from at least three distinct passes over the same set of sources:

(1) Fresh emissions inserted into that day's sea breeze,

(2) Overnight emissions from coastal point sources inserted into the previous evening's land breeze, and

(3) Urban backwash due in part to coastline emissions transported inland during the previous day's sea breeze regime.

A total sulfur balance on air parcels observed at a receptor point in coastal Los Angeles County then yields the expression that:

$$S_{total_j} = S_{backwash_j} + S_{overnight_j} + S_{fresh_j} + S_{marine_j} \quad (1)$$

where

S_{total_j} is total sulfur oxides concentration stated as elemental sulfur observed during time interval j;

$S_{backwash_j}$ is that portion of S_{total_j} due to recirculation of pollutants previously located over the urban area upwind of our receptor point during the land breeze regime;

$S_{overnight_j}$ is that portion of S_{total_j} due to overnight emissions from coastal point sources downwind of our receptor point during the land breeze regime;

S_{fresh_j} is that portion of S_{total_j} due to fresh pollutant emissions upwind of our receptor point during that day's sea breeze regime;

S_{marine_j} is that portion of S_{total_j} arising from intrusion of marine air masses over land for the first time after the backwash material has been cleared from Santa Monica Bay by continuation of a sea breeze stronger than the prior night's land breeze.

A similar expression is written for total sulfur appearing as sulfate in each air parcel:

$$SO_{4_{total_j}} = SO_{4_{backwash_j}} + SO_{4_{overnight_j}} + SO_{4_{fresh_j}} + SO_{4_{marine_j}} \quad (2)$$

where

$SO_{4_{total_j}}$ is total sulfate concentration stated as sulfur observed during time interval j;

$SO_{4_{backwash_j}}$ is that portion of $SO_{4_{total_j}}$ due to recirculation of pollutants located over the urban area upwind of our receptor point during the land breeze regime.

$SO_{4_{overnight_j}}$ is that portion of $SO_{4_{total_j}}$ due to overnight emissions from coastal point sources downwind of our receptor point during the land breeze regime;

$SO_{4_{fresh_j}}$ is that portion of $SO_{4_{total_j}}$ due to fresh pollutant emissions upwind of our receptor point during that day's sea breeze regime;

$SO_{4_{marine_j}}$ is that portion of $SO_{4_{total_j}}$ arising from intrusion of marine air masses over land for the first time.

3.0 Experimental Program Relevant to Sulfur Oxides Transport and Transformation

An experimental program was undertaken during July, 1977, in an attempt to separate each of these contributors to local sulfur oxides air quality. Sulfate concentrations were measured at two hour intervals by low-volume sampling at two onshore locations: Redondo Beach and Lennox. Samples were collected on Gelman GA-1 glass fiber filters and analyzed for total sulfur (reported as sulfate) by the X-ray fluorescence method (Tsou et al., 1977). The monitoring site at Lennox was co-located with the South Coast Air Quality Management District's SO_2 continuous monitoring station in that community. A time history of sulfate, sulfur dioxide and total sulfur oxides air quality, S_{total}, thus can be constructed at that location. For that reason, our analysis will focus on Lennox as the receptor point of interest.

Sulfur oxides concentrations in offshore marine air were sampled by a variety of methods. A sulfate sampling station similar to the ones at Redondo Beach and Lennox was established at Santa Catalina

Island off of the Southern California coast. Flame photometric total sulfur analyzers were located at Santa Catalina Island and aboard the research vessel Acania as it cruised in the Santa Monica Bay. From this sampling program, offshore sulfur oxides concentrations, S_{marine}, could be determined.

Surface wind speed and direction measurements obtained from the South Coast Air Quality Management District's Redondo Beach and Venice stations were used to track the outflow and return of urban backwash air masses. Measurements of inversion base height over the Santa Monica Bay were obtained from an acoustic sounder located aboard the Acania. From pollutant measurements made at Lennox during the nighttime land breeze regime, the initial concentrations of SO_2 and sulfates in the backwash air masses were determined as those air masses moved seaward. Meteorological data then can be used to estimate that portion of S_{total} observed at Lennox during the next sea breeze period that originated in the previous night's backwash from the urban area.

In order to identify the contribution to S_{total} due to overnight emissions from coastal point sources, sulfur hexafluoride tracer was injected into the stack of unit number 4 at Southern California Edison Company's El Segundo power plant. A total of 90 Kg of SF_6 was released at a continuous rate beginning at 2400 hours Pacific Daylight Time (PDT) on July 21, 1977, and ending at 500 hours on the morning of July 22, 1977. Those tracer-labeled emissions blown out to sea at night were then observed to recross the coastline during the following day's land breeze. By considering the tracer concentration

observed near Lennox and the ratio of tracer released to sulfur oxides emitted by El Segundo point sources, the impact of overnight emissions from those sources on the following day's air quality at Lennox can be estimated.

Experimental means have been described which identify total sulfur oxides concentrations, S_{total}, plus the contributions to that total from urban backwash, overnight emissions and marine air quality. From equation (1), we see that the remaining term which reflects the effect of direct transport of fresh sulfur oxides emissions from sources upwind of Lennox in the morning can be determined by difference.

4.0 Data and Analysis

Sulfate air quality measurements made at Lennox, Redondo Beach, and Santa Catalina Island are shown in Figure 2. From July 19 through July 26, sulfate concentrations at Catalina averaged 8.9 μ gm/m^3 (as $SO_4^=$). A long term fluctuation about that mean value is apparent, with an amplitude of approximately ± 5 μ gm/m^3 and period of about one week. The major departure from that pattern occurs in the afternoon of July 24, when sulfate concentrations at Catalina increased sharply from 9.0 μ gm/m^3 up to 27.4 μ gm/m^3 over a two hour time interval. Sulfur hexafluoride samplers located at Catalina indicate that SO_x emissions accompanied by a tracer release made the previous night at El Segundo passed over Catalina at that time. That was the only occasion on which transport from El Segundo to Catalina was demonstrated during this study.

Sulfate measurements made at Lennox and Redondo Beach show a distinct enrichment in pollutant concentrations above the baseline

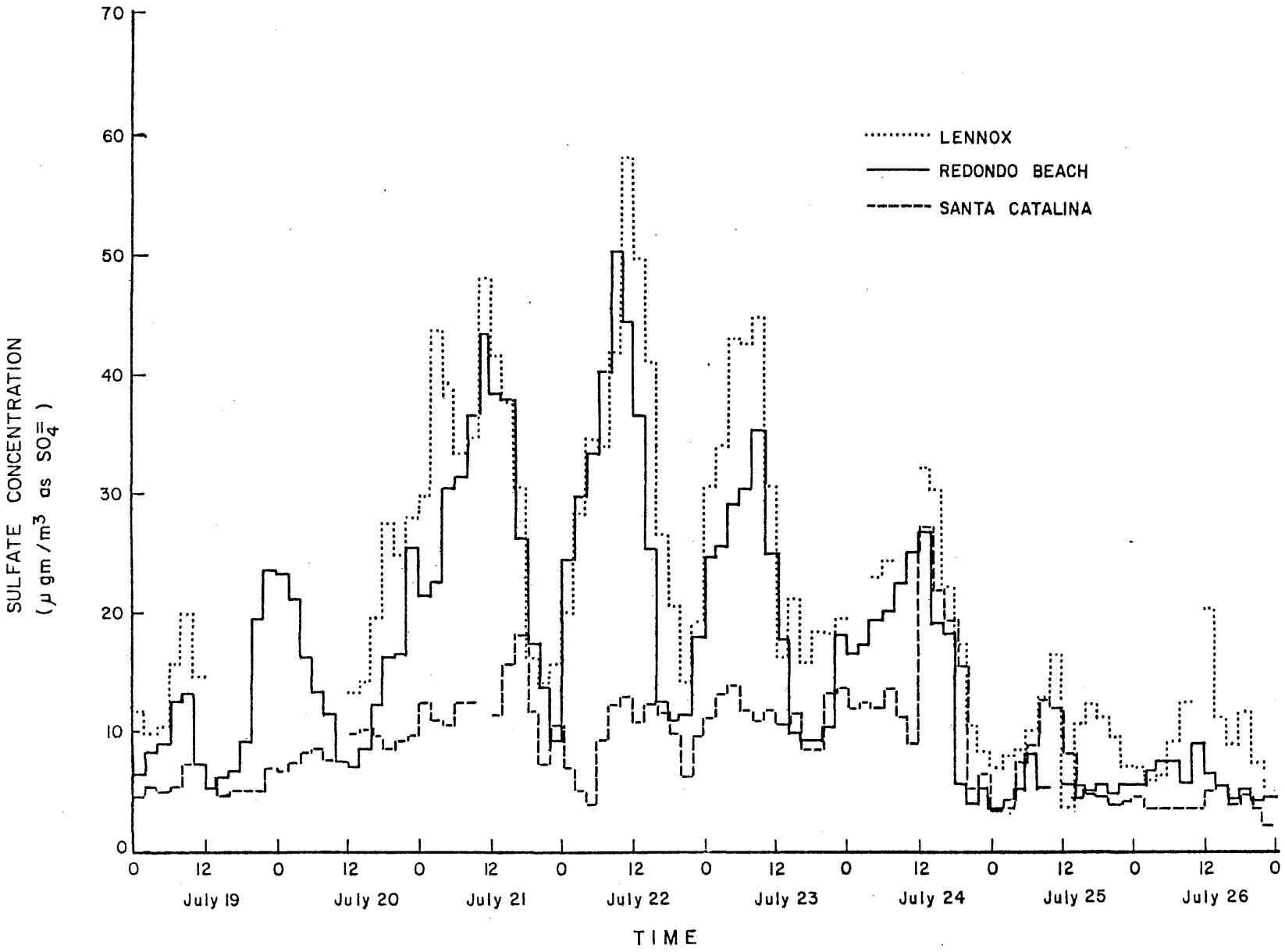
70
60
50
40
30
20
10
0
SULFATE CONCENTRATION
(μ gm/m³ as $SO_4^{=}$)
LENNOX
REDONDO BEACH
SANTA CATALINA
0
12
0
12
0
12
0
12
0
12
0
12
0
12
0
12
0
July 19
July 20
July 21
July 22
July 23
July 24
July 25
July 26
TIME

Figure 2

formed by marine air quality. A strong diurnal variation in sulfate concentrations is observed, with peak values typically occurring at about noontime, followed by a decline to near Santa Catalina Island levels for a short time at night. A longer term pattern to onshore air quality is also observed which tends to follow that at Catalina. Successively rising daily maximum sulfate concentrations are observed from July 19 through July 22, followed by a subsequent decline over a period of several days. Sulfate concentrations at Lennox and Redondo Beach track each other closely over time.

Sulfur balance calculations will be used to explore the origin of the highest sulfate concentrations observed at Lennox. Figures 2 and 3 show that both sulfate and sulfur dioxide concentrations at Lennox peaked strongly between 1000 and 1200 hours on the morning of July 22, 1977. However, in order to explain the factors contributing to that peak, one must return to the later hours of the previous day. Just before noon on July 21st, sulfate air quality peaked at Lennox. Then throughout that afternoon and evening, sulfate concentrations declined as wind speed increased and as material stored over Santa Monica Bay was transported inland by the sea breeze.

By 2200 hours on July 21, sulfate concentrations at Lennox and Redondo Beach had fallen to near the levels observed at Santa Catalina Island. Then the land breeze began at 2300 hours PDT on that day. At this time, polluted air masses previously over land began to flow backward out to sea. A dividing line between marine air and the urban

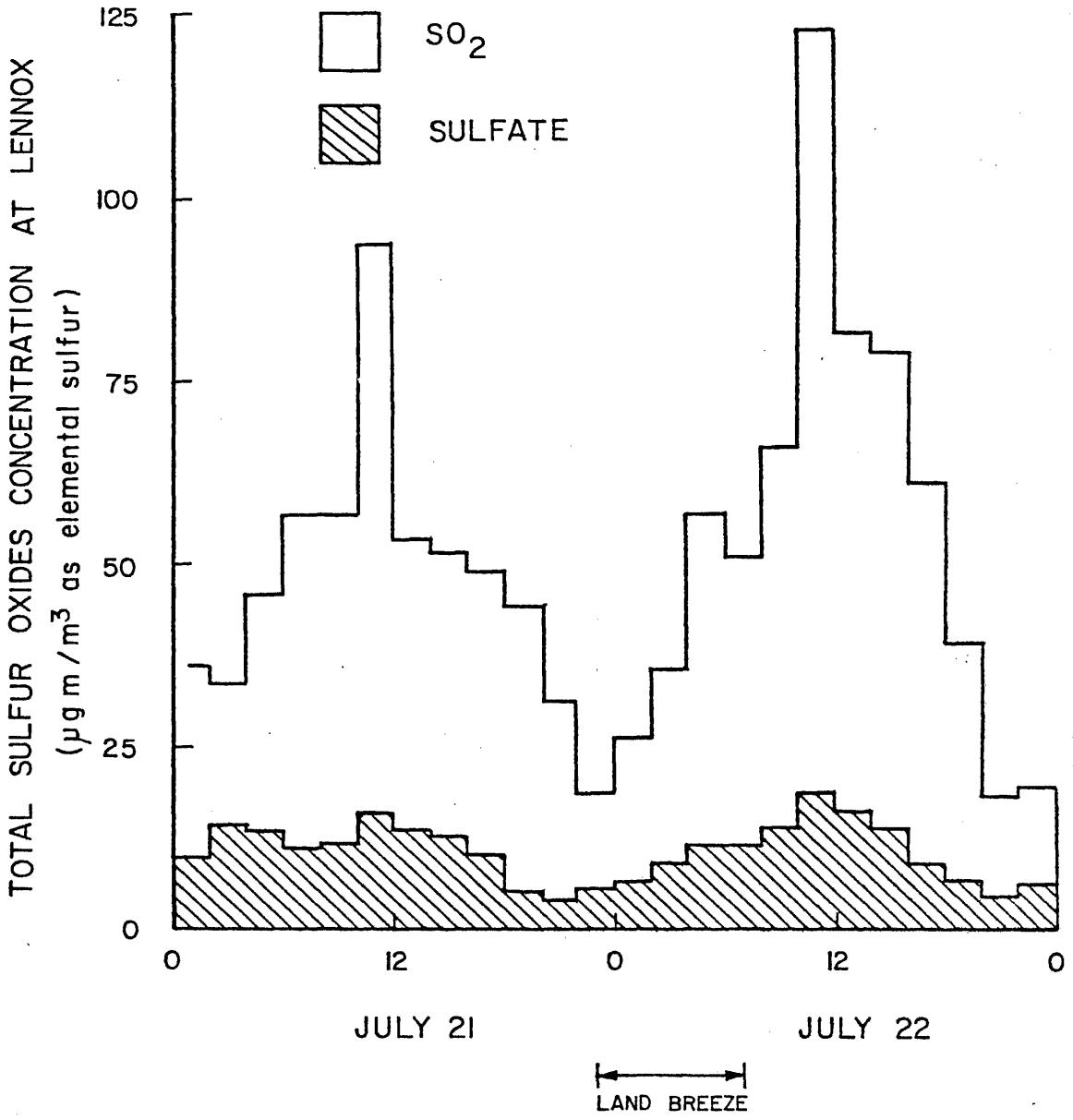
TOTAL SULFUR OXIDES CONCENTRATION AT LENNOX
(μg m/m³ as elemental sulfur)
125
100
75
50
25
0
SO2
SULFATE
0
12
0
12
0
JULY 21
JULY 22
LAND BREEZE

Figure 3

backwash is established at the coast with the onset of the land breeze and propagates seaward.

4.1 Backwash Air Quality

As the material which was stored over land recrosses the Lennox monitoring site, Figure 2 shows that sulfate concentrations began to increase in a near "mirror image" of the previous evening's inland progression. This pattern is consistent with that which would be expected if the same air mass passed back and forth over the same monitoring site with relatively little mixing in the direction of the flow.

Consider an x-y coordinate system with the y-axis parallel to the Santa Monica Bay coastline. The motion of air normal to the coast is measured along the x axis with x = 0 referring to the coordinate of the air monitoring station at Lennox.

Beginning with the onset of the land breeze at night, the seaward penetration, Δx_i, of urban backwash air masses during each time interval, i, was calculated from the separate averages of wind speeds and wind directions observed at Venice and Redondo Beach. Inversion base data from the acoustic sounder aboard the Acania were used to obtain the depth, h_i, of the mixed layer at that time. Air parcels of seaward extent Δx_i, height h_i and semi-infinite length in the crosswind direction were successively placed over the Santa Monica Bay.

As each air mass so defined passes over the Lennox air monitoring station, initial conditions for total sulfur concentration existing

as sulfur dioxide, $S_{SO_{2B_i}}(0)$, and sulfates, $S_{SO_{4B_i}}(0)$, are established, as given in lines 2 through 5 of Table 1. It is assumed that these aged air masses are vertically well mixed to the base of the inversion. Comparison of sulfate data taken at Redondo Beach and Lennox from late July 21 through the morning of July 22 indicates that crosswind concentration gradients on this occasion were small (see Figure 2). Consequently, crosswind diffusion of backwash air parcels will be neglected, and calculations will be performed for a two dimensional system.

Surface wind data indicate that a land breeze started between 2300 and 2400 hours on July 21. At 2320 hours on July 21, the inversion base was located at 290 meters above sea level, and the backwash material was taken to be well mixed at least to that altitude at that time. From 2400 hours on July 21 until the late afternoon of July 22, inversion base height over the ocean averaged 189 meters above sea level and never rose to more than 260 meters above sea level. From these data it is concluded that the inversion base never rose high enough to include portions of the atmosphere free of backwash material, and that changes in inversion height provided no opportunity for vertical dilution of backwash or marine air parcels.

While dilution overnight would be ineffective in reducing SO_2 and sulfate concentrations, sulfur oxides concentrations could be changed by chemical reaction. SO_2 residing below the inversion base may react to form sulfates, and may be depleted by deposition at the ground or ocean's surface. The following set of competitive first

TABLE 1

Sulfur Oxides Concentrations in Air Parcels Passing Lennox with Comparison to Marine Air Quality

Origin	Date	Hours PDT	Index[c]	SO_2[d] (ppm)	SO_2 as Elemental Sulfur ($\mu gm/m^3$)	$SO_4^=$ ($\mu gm/m^3$)[e]	$SO_4^=$ as Elemental Sulfur ($\mu gm/m^3$)	Total Sulfur ($\mu gm/m^3$)[f]
Marine[a]	July 21	2300	i=1		4.2	10.7	3.6	7.8
Urban Backwash[b]	July 21	2200 - 0000	i=2	0.010	13.1	15.5	5.2	18.3
Urban Backwash	July 22	0000 - 0200	i=3	0.015	19.6	20.2	6.7	26.3
Urban Backwash	July 22	0200 - 0400	i=4	0.020	26.2	28.3	9.4	35.6
Urban Backwash	July 22	0400 - 0600	i=5	0.035	45.8	34.5	11.5	57.3
Land Breeze/Sea Breeze Transition	July 22	0600 - 0800	*	0.030	39.2	34.0	11.3	50.5
Inflow from Seaward	July 22	0800 - 1000	j=1	0.040	52.3	41.8	13.9	66.2
Inflow from Seaward	July 22	1000 - 1200	j=2	0.080	104.6	58.0	19.3	123.9
Inflow from Seaward	July 22	1200 - 1400	j=3	0.050	65.4	49.9	16.6	82.0
Inflow from Seaward	July 22	1400 - 1600	j=4	0.050	65.4	41.0	13.7	79.1
Inflow from Seaward	July 22	1600 - 1800	j=5	0.040	52.3	26.6	8.9	61.2
Inflow from Seaward	July 22	1800 - 2000	j=6	0.035	45.8	20.6	6.9	52.7
Inflow from Seaward	July 22	2000 - 2200	j=7	0.015	19.6	14.1	4.7	24.3
Sea Breeze/Land Breeze Transition	July 22	2200 - 2300	j=8	0.010	13.1	19.2	6.4	19.5

Notes:

(a) Marine air quality as measured at Santa Catalina Island is assumed to extend throughout Santa Monica Bay at this time. All other pollutant concentrations shown were measured at Lennox.

(b) An air parcel with this chemical composition is assumed to extend from Lennox to the Santa Monica Bay coastline at the onset of the land breeze at 2300 hours PDT July 21.

(c) A time interval index, i, is used to indicate the initial condition of an air parcel transported seaward during the land breeze. A time interval index, j, indicates this condition of air parcels advected inland past Lennox by the next day's sea breeze.

(d) With the exception of the marine data which was inferred from Tsou et al. (1977), SO_2 concentrations are taken from South Coast Air Quality Management District monitoring records at Lennox. SO_2 concentrations occurring between 11 a.m. and noon PDT July 22 had to be estimated from examination of a strip chart recording covering portions of that hour.

(e) Sulfate data and marine total sulfur data are from measurements by Tsou et al. (1977).

(f) $\mu gm/m^3$ as elemental sulfur

order reaction processes were used to model this chemical transformation and pollutant deposition:

$$\frac{d\, S_{SO_{2B}}}{dt} = -k\, S_{SO_{2B}} - \frac{V_g}{h} S_{SO_{2B}} \qquad (3)$$

where

$S_{SO_{2B}}$ is the sulfur oxides concentration existing as sulfur dioxide within an urban backwash air parcel;

k is the overall rate of oxidation of SO_2 to form sulfates due to homogenous and heterogeneous processes combined;

V_g is the deposition velocity for SO_2 at the earth's surface;

h is the depth of the mixed layer below the inversion base.

In a similar fashion, expressions for sulfate formed can be written as

$$\frac{d\, S_{SO_{4B}}}{dt} = k\, S_{SO_{2B}} \qquad (4)$$

where

$S_{SO_{4B}}$ is sulfur oxides concentration existing as sulfate within an urban backwash air parcel.

Studies of sulfate deposition velocity made in the Los Angeles Basin by Davidson (1977) indicate that particulate sulfates are present predominantly in submicron size ranges, and thus exhibit extremely low dry deposition rates. Ground level deposition of sulfates thus is neglected in equation 4. Sulfur dioxide gas, on the other hand, undergoes comparatively rapid removal at the earth's surface. A sulfur dioxide deposition velocity of 0.7 cm/sec is estimated from Garland (1974).

Solving equations 3 and 4 over a time interval from t to $t+\Delta t$ yields,

$$S_{SO_{2B}}(t+\Delta t) = S_{SO_{2B}}(t)\left[e^{-k(1+\frac{V_g}{kh})\,\Delta t}\right] \tag{5}$$

$$S_{SO_{4B}}(t+\Delta t) = S_{SO_{4B}}(t) + S_{SO_{2B}}(t)\left[\frac{1}{1+\frac{V_g}{kh}}\right]\left[1-e^{-k(1+\frac{V_g}{kh})\,\Delta t}\right] \tag{6}$$

As indicated by the dimensionless group (V_g/kh), in order for the SO_2 in the backwash air masses to make a significant contribution to the total sulfate concentration observed at Lennox the next day, the overall rate of SO_2 oxidation must have a value of order (V_g/h) or (in this case) a value of a few percent per hour.

A convenient way of describing the temporal relationship between air parcels sent seaward at night and those returning the next morning with the sea breeze is by means of a "folded time line", as shown in Figure 4. If viewed from the start of the sea breeze at 0700 hours on July 22, the lower axis of that graph would give the location of the boundaries of those air parcels transported seaward during the previous land breeze. In this case, pollutants have been transported seaward to a distance of 30.0 km from the coast or a distance x = -35.5 km from Lennox (which is located 5.5 km inland). If air parcels are assumed to return past Lennox on a last-in first-out basis, then the upper axis of Figure 4 represents the inland progression caused by the sea breeze on July 22. It is seen, for example, that part of the

Figure 4

FOLDED TIME LINE

SHOWING CORRESPONDENCE BETWEEN LAND BREEZE
AND SEA BREEZE AIR PARCELS — JULY 22, 1977

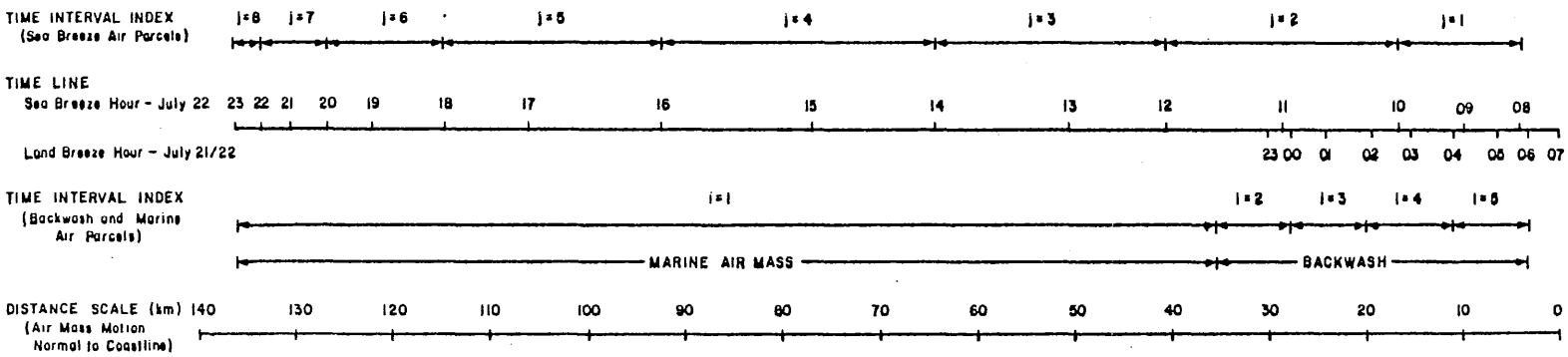

air parcel passing Lennox between 2300 hours and midnight on July 21, plus all of the air masses passing between midnight and 0200 hours on July 22, plus part of the air mass passing Lennox between 0200 and 0300 hours on July 22 returned back over Lennox between 1000 and 1100 hours on the morning of July 22.

The contribution to the total sulfur oxides concentration observed at Lennox due to the urban backwash at any time interval, j, is the sum of total sulfur oxides originally in the backwash less that portion of the SO_2 in the backwash which deposited at the ocean's surface. Since the sea breeze is typically stronger than the land breeze, polluted air parcels transported seaward during several time periods the previous night may contribute to backwash concentrations sampled over land during a single time interval the next morning. That is,

$$S_{\text{backwash}_j} = \sum_{i=1}^{n} \alpha_{ij} \left[S_{SO_{4B_i}}(0) + S_{SO_{2B_i}}(0) \left[1 - \frac{\frac{V_g}{kh}}{\left(1 + \frac{V_g}{kh}\right)} \left(1 - e^{-k\left(1+\frac{V_g}{kh}\right)\Delta t_{ij}} \right) \right] \right] \quad (7)$$

where the newly introduced terms are

α_{ij} the fraction of the backwash air parcel characterized during land breeze time interval i which recrosses Lennox during the sea breeze time interval j;

Δt_{ij} the retention time for each air parcel between initial characterization and subsequent return.

For the purposes of our calculations, some approximations were made. The value of Δt_{ij} was taken as the time that the centroid of the air parcel (which travels seaward during the i^{th} time interval and returns

during the $j^{\underline{th}}$ time interval) spent west of Lennox. The inversion base height, h, was taken to be constant and equal to its average value of 189 meters above sea level.

In a similar fashion, the backwash contribution to sulfate concentration observed at Lennox during any time interval j was computed as follows:

$$SO_{4_{backwash_j}} = \sum_{i=1}^{n} \alpha_{ij} \left[SO_{4B_i}(0) + SO_{2B_i}(0) \left(\frac{1}{1+\frac{V_g}{kh}} \right) \left(1 - e^{-k\left(1+\frac{V_g}{kh}\right)\Delta t_{ij}} \right) \right] \tag{8}$$

4.2 Marine Air Quality

By the end of the sea breeze at 2300 hours on July 21, sulfate concentrations at Redondo Beach and Lennox had dropped to near the levels recorded at Santa Catalina Island. A large mass of marine air of uniform composition was assumed to completely fill the Santa Monica Bay at that time. Measurements made at Santa Catalina Island between 2300 hours and midnight indicated a total sulfur oxides concentration in marine air of 0.006 ppm (or 7.8 $\mu gm/m^3$ as sulfur) which included 10.7 $\mu gm/m^3$ of sulfates (3.6 $\mu gm/m^3$ as sulfur). Simultaneous measurements made aboard the Acania indicated a total sulfur concentration of 0.01 ppm in air over the Santa Monica Bay, which is consistent with the Catalina data to within the number of significant figures given.

This marine air mass residing over the Santa Monica Bay was pushed seaward by the land breeze during the early morning hours of

July 22. Thus once the urban backwash had been withdrawn completely from over the Santa Monica Bay on the morning of July 22, marine air parcels would begin to appear over land. The initial chemical composition of each marine air mass was taken to be like that observed at Catalina Island at 2300 hours on July 21, as given in line 1 of Table 1. The residence times for SO_2 oxidation and deposition were taken from this initial condition at 2300 hours on July 21 until the time of arrival at Lennox of the midpoint of the air parcel of interest.

The effect of residence time on the sulfur oxides concentrations contained in marine air was computed by the same procedure as described for the backwash air parcels. That is,

$$S_{\text{marine}_j} = \sum_{i=1}^{n} \alpha_{ij} \left[S_{SO_{4M_i}}(0) + S_{SO_{2M_i}}(0) \left[1 - \frac{\frac{V_g}{kh}}{\left(1 + \frac{V_g}{kh}\right)} \left(1 - e^{-k\left(1 + \frac{V_g}{kh}\right)\Delta t_{ij}} \right) \right] \right] \tag{9}$$

and

$$SO_{4_{\text{marine}_j}} = \sum_{i=1}^{n} \alpha_{ij} \left[S_{SO_{4M_i}}(0) + S_{SO_{2M_i}}(0) \left(\frac{1}{1 + \frac{V_g}{kh}} \right) \left(1 - e^{-k\left(1 + \frac{V_g}{kh}\right)\Delta t_{ij}} \right) \right] \tag{10}$$

where the newly introduced terms are:

$S_{SO_{2M_i}}(0)$ the initial condition for total sulfur existing as sulfur dioxide in marine air at time interval i;

$S_{SO_{4M_i}}(0)$ the initial condition for total sulfur existing as sulfates in marine air at time interval i.

Analysis of backwash and marine air motion coefficients, α_{ij}, and residence times, Δt_{ij}, are given in Table 2. The values of α_{ij} and Δt_{ij} are conveniently estimated from the folded time line in Figure 4.

4.3 Overnight Emissions

Overnight emissions into the land breeze from point sources at El Segundo were tagged with SF_6 tracer. From tracer measurements made aboard the Acania, it was found that emissions from these elevated sources stayed aloft until about 5:30 a.m., after which fumigation to the ocean's surface occurred within a few minutes over a wide area of Santa Monica Bay.

Trajectories calculated from surface winds would indicate that emissions sent seaward at night tacked northward before recrossing the coastline the next morning. However, from a line of closely spaced SF_6 samplers located at the coast, it was observed that the peak returning SF_6 concentration (76 ppt hourly average) occurred between 1000 and 1100 hours *at the El Segundo monitoring site.* That value compares favorably to the highest hourly average SF_6 concentration observed aboard the Acania (82 ppt between 0900 and 1000 hours July 22) as the ship sailed along a line headed almost directly westward from a point located several miles off of El Segundo. The implication is that the zone of highest impact of overnight emissions from Santa Monica Bay point sources recrossed the coastline the next morning near the point of pollutant origin.

The concentration of sulfur oxides later observed at Lennox due to overnight emissions was therefore estimated from measured tracer

concentrations plus a knowledge of the ratio of El Segundo SO_x emissions to SF_6 tracer emissions. While resident aloft, SO_2 in the elevated source plume can react to form sulfates, but no removal processes occur due to deposition at the earth's surface. After fumigation, surface deposition and SO_2 oxidation serve to alter pollutant composition and concentration. Total sulfur oxides concentrations observed at Lennox the next morning due to overnight emissions from El Segundo were taken to be equal to that computed from tracer concentrations and the SF_6 tracer to SO_x mass ratio, less any SO_2 surface deposition. That is,

$$S_{\text{overnight}_j} = \beta \cdot [SF_6]_j \left[1 - \left[(1 - f_s)\left(e^{-k\Delta t_{aj}}\right)\left(\frac{\frac{V_g}{kh}}{1+\frac{V_g}{kh}}\right)\left(1 - e^{-k\left(1+\frac{V_g}{kh}\right)\Delta t_{bj}}\right)\right]\right] \tag{11}$$

where the newly defined terms are:

β — the mass ratio of SF_6 tracer emissions to El Segundo point source SO_x emissions.

$[SF_6]_j$ — the mass concentration of SF_6 tracer estimated to be at Lennox during morning time interval j. This estimate was based upon measurements made upwind at El Segundo one hour earlier.

f_s — the volume fraction of SO_x emissions present as sulfates at the exit of the stack.

Δt_{aj} — the time interval from the release of pollutants from elevated sources to the time at which fumigation occurred, for material observed at Lennox during time interval j.

Δt_{bj} — the time from fumigation until that air mass recrossed Lennox during time interval j.

TABLE 2

Analysis of Air Motion Coefficients and Residence Times for Backwash and Marine Air Parcels

1. Air Motion Coefficient Matrix

α_{ij} — j →, i ↓

i \ j	1	2	3	4	5	6	7	8
1	0	0.23	1.0	1.0	1.0	1.0	1.0	1.0
2	0	0.30	0	0	0	0	0	0
3	0	0.35	0	0	0	0	0	0
4	0.44	0.12	0	0	0	0	0	0
5	0.56	0	0	0	0	0	0	0

2. Residence Time Matrix (hours)

Δt_{ij} — j →, i ↓

i \ j	1	2	3	4	5	6	7	8
1	-	12.8	14	16	18	20	22	23.5
2	-	12.2	-	-	-	-	-	-
3	-	9.4	-	-	-	-	-	-
4	6.2	7.8	-	-	-	-	-	-
5	3.9	-	-	-	-	-	-	-

3. Interpretation:

For example, during time interval j=1 (between 8 and 10 a.m. on July 22 as shown in Table 1) 56% of the air masses passing over Lennox had initial chemical composition like those sent seaward over Lennox during time interval i=5 (between 4 and 6 a.m. on July 22 as shown in Table 1). The average residence time for that material was Δt_{51} = 3.9 hours.

In a similar fashion, the contribution to daytime sulfate air quality due to overnight emissions from coastal point sources, $SO_{4_{overnight_j}}$, can be determined. It is composed of an increment due to the primary emissions of sulfates from those sources, plus sulfates formed from SO_2 oxidation during the period while the plumes were isolated aloft, plus sulfates formed from SO_2 oxidation after the plumes had fumigated to the ocean's surface:

$$SO_{4_{overnight_j}} = \beta \cdot [SF_6]_j \left[f_s + (1 - f_s)\left(1 - e^{-k\,\Delta t_{aj}}\right) \right]$$

$$+ \beta \cdot [SF_6]_j [1 - f_s] \left[e^{-k\,\Delta t_{aj}} \right] \left[\frac{1}{1 + \frac{V_g}{kh}} \right] \left[1 - e^{-k \left(1 + \frac{V_g}{kh}\right) \Delta t_{bj}} \right] \tag{12}$$

The initial fraction of SO_x emissions, f_s, evolved directly as sulfates from utility fuel combustion and refinery processes is taken as 0.03 or 3% of total SO_x emissions based on data given by Hunter and Helgeson (1976). The mass ratio of El Segundo sulfur oxides emissions to SF_6 released on the early morning of July 22 is estimated in Table 3 and cross-checked in Table 4 against the SF_6 and SO_x increments observed over the ocean after plume downmixing.

Mass balance calculations for SF_6 release and return are shown in Figure 5. In order to estimate Δt_{aj} and Δt_{bj}, the midpoint of time interval j at Lennox was chosen for reference. Since the SF_6 monitors were located at El Segundo upwind of Lennox, an estimate of the

TABLE 3

Ratio of Overnight Emissions from Elevated Point Sources at El Segundo to SF_6 Released at that Location

SO_x Source		Generating Capacity (Megawatts)	Average Load Factor 0000 to 0500 hrs July 22, 1977	Fuel Oil Burned (Barrels)	Fuel Oil Sulfur Content (wt %)	Total SO_x Emissions Over 5 Hour Period (Kilograms of Elemental Sulfur)
SCE El Segundo Power Plant	Unit 1	175	0.097	135	0.22	42.9
	Unit 2	175	0.297	413	0.22	131.2
	Unit 3	335	0.582	1551	0.22	492.7
	Unit 4	335	0.573	1527	0.22	485.1
LADWP Scattergood Power Plant	Unit 1	179	0.485	690	0.35	348.7
	Unit 2	179	0.0	0	--	--
	Unit 3	gas fired only		0	--	--
Chevron El Segundo Refinery						523.5
					Subtotal	2024.1

SF_6 Source		Total SF_6 Released Over 5 Hour Period (Kg as SF_6)
SCE El Segundo Power Plant	Unit 4	90

Ratio of SO_x to SF_6

Total Sulfur to SF_6 ratio = 22.5 : 1 on a mass basis
SO_x to SF_6 ratio = 103 : 1 on a volume basis
$\therefore$ 1 ppt SF_6 ≈ 0.000103 ppm SO_x

Notes:

El Segundo load factors and fuel sulfur content from communication with plant personnel during SF_6 release.

Scattergood load factors and sulfur content from McCullough (1978).

Fuel burned and SO_x emissions calculated from unit generating capacity and load factors assuming:
Heat Rate = 10,000 BTU/KWH
Fuel Oil Energy Content = 6.287×10^6 BTU/bbl
Fuel Oil Gravity = 24° API or 144.4 kg/bbl

Chevron El Segundo Refinery emissions estimated over 5 hour period at 5/24^{ths} of that plant's 1976 average daily emission rate of 5540 lbs/day as elemental sulfur (given by the South Coast Air Quality Management District's 1976 sulfur balance on that facility).

TABLE 4

Ambient Monitoring Confirmation of the Ratio
of Elevated Source SO_x Emissions to SF_6 Released

Time	Hourly Average of Simultaneous Observations of SO_x and SF_6 Concentrations Along the Ship Track of the Acania	
	SF_6 in ppt	SO_x in ppm
0600 to 0700 hours July 22	6.6	0.01
0700 to 0800 hours July 22	59.6	0.02
0800 to 0900 hours July 22	33.1	0.02
0900 to 1000 hours July 22	82.0	0.02
1000 to 1100 hours July 22	43.6	0.02

Observation: Addition of (82.0 - 6.6) = 75.4 ppt of SF_6 was accompanied by an increase in SO_x of about 0.01 ppm.

Inferred ratio of SF_6 to SO_x is:

1 ppt SF_6 ≃ 0.000133 ppm SO_x, which is very close to the ratio estimate from Table 3.

Figure 5

SF_6 TRACER
CUMULATIVE RELEASE AND RETURN

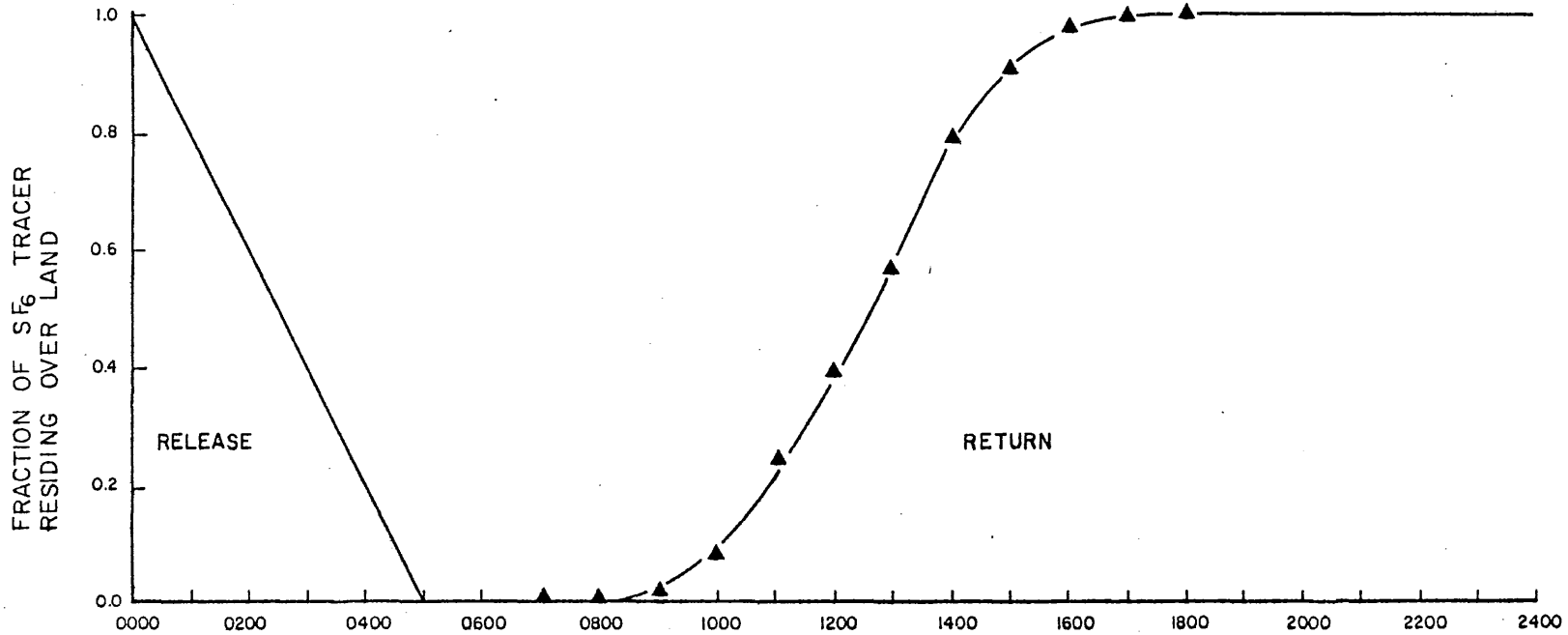

TIME OF RELEASE AND SUBSEQUENT RETURN PAST THE COASTLINE
HOURS PACIFIC DAYLIGHT TIME - JULY 22, 1977

TIME INTERVAL	0800-1000	1000-1200	1200-1400	1400-1600	1600-1800	(HOURS PDT)
INDEX	j=1	j=2	j=3	j=4	j=5	

Next Closest Time Interval For Return Past Lennox
(Located Inland From The Coast)

concentration and cumulative amount of SF_6 having passed Lennox at the midpoint of time interval j was read from the midpoint of the next earlier sampling interval measured at El Segundo. Then the midpoint time of release of that SF_6-labeled material was determined by reading horizontally across to the cumulative release graph on the left hand side of Figure 5, assuming that air parcels return from over the Santa Monica Bay on a last-in first-out basis. The time interval from release to return is $\Delta t_j = \Delta t_{aj} + \Delta t_{bj}$. From a knowledge of the time at which overnight emissions mixed down to the ocean's surface, subdivision of Δt_j into Δt_{aj} and Δt_{bj} is accomplished (see Table 5.)

4.4 Fresh Emissions

Fresh emissions occurring after the end of the SF_6 tracer release also influenced Lennox air quality. An analysis of wind flow data on the morning of July 22 indicated that emissions into the sea breeze at El Segundo were transported directly toward Lennox with transport times as shown in Table 6. The contribution to Lennox sulfur oxides air quality due to fresh emissions from sources in the vicinity of that monitoring site was taken to be equal to the difference between total SO_x observed and contributions from other known sources. That is,

$$S_{fresh_j} = S_{total_j} - S_{backwash_j} - S_{marine_j} - S_{overnight_j} \qquad (13)$$

The maximum sulfate contribution due to fresh emissions from nearby sources is taken to be

$$SO_{4_{fresh_j}} = S_{fresh_j} \cdot (f_s + (1 - f_s)(1 - e^{-k \Delta t_{cj}})) \qquad (14)$$

TABLE 5

Analysis of Concentration and Residence Times
for SF_6-Labeled Air Parcels

Time Interval for SO_x Sampling at Lennox July 22	Time Interval Index	Closest Comparable Time Interval for SF_6 Sampling in That Air Mass at El Segundo	SF_{6_j} (PPT)	Cumulative Quantity of SF_6 Release Returned Past Samplers by Mid-Point of That Time Period	Estimated Time at Mid-Point of Air Parcel Release PDT	Time at Mid-Point of Sea Breeze Sampling Interval at Lennox PDT	Estimated Retention Time From Release to Receipt at Lennox		
							Total Δt_j (hours)	Elevated Plume Period Δt_{aj} (hours)	Period Following Down-Mixing Δt_{bj} (hours)
0800 - 1000 hrs	j = 1	0700 - 0900 hrs	3.0	1 %	0457 hrs	0900 hrs	4.05	0.55	3.50
1000 - 1200 hrs	j = 2	0900 - 1100 hrs	41.5	6.3%	0441 hrs	1100 hrs	6.32	0.82	5.50
1200 - 1400 hrs	j = 3	1100 - 1300 hrs	30.0	39 %	0303 hrs	1300 hrs	9.95	2.45	7.50
1400 - 1600 hrs	j = 4	1300 - 1500 hrs	7.5	79 %	0103 hrs	1500 hrs	13.95	4.45	9.50
1600 - 1800 hrs	j = 5	1500 - 1700 hrs	2.0	98.5%	0004 hrs	1700 hrs	16.93	5.43	11.50

TABLE 6

Transport Times from El Segundo to Lennox
during Sea Breeze Regime, July 22, 1977

Time Interval (Hours, PDT)	Time Interval Index	Wind Speed (m/sec)	Direction (Degrees from Due North)	Transit Time to Lennox (hours)
0800 - 1000	j=1	1.68	240°	0.92
1000 - 1200	j=2	3.35	240°	0.46
1200 - 1400	j=3	3.35	240°	0.46
1400 - 1600	j=4	3.93	∿240°	0.39
1600 - 1800	j=5	3.13	∿240°	0.49
1800 - 2000	j=6	1.65	∿240°	0.93
2000 - 2200	j=7	1.00	∿260°	1.64
2200 - 2300	j=8	0.90	∿275°	2.09

Note: Lennox is located 5.54 km from El Segundo. A wind direction of 240° yields direct transport from El Segundo to Lennox.

assuming that these emissions occurred from elevated sources so close to the receptor point that ground level deposition can be neglected during most of the transport time from source to receptor. It was assumed that the principal source of these emissions was from El Segundo, and thus that transport times, Δt_{cj}, would be taken from Table 6.

4.6 Sulfur Balance Calculations

Expressions 7, 9, 11 and 13 were substituted into equation 1, while equations 8, 10, 12, 14 were substituted into equation 2. The result is a system of two sulfur balance equations involving two unknowns, S_{fresh_j} and the effective average SO_2 oxidation rate, k. At each time interval j, a trial value for k was assumed. The total sulfur balance (equation 1) was used to calculate S_{fresh_j}. That value of S_{fresh_j} was inserted into the sulfate balance (equation 2) and an estimate of $SO_{4_{total_j}}$ was obtained and compared to the measured value of $SO_{4_{total_j}}$. The system of equations was solved by successive substitution of k values until measured and calculated sulfate concentrations agreed.

5.0 Discussion of Results

From solution of our system of sulfur balance equations, a series of estimates were made of the rate of SO_2 oxidation within air parcels arriving at Lennox on July 22. In every case, the estimated value for k was significantly greater than zero, indicating that sulfate formation was occurring over time.

In Table 7, individual determinations of k are compared to experimental results obtained in the Los Angeles atmosphere by Roberts (1975) during the same season of a previous year. The results of the

TABLE 7

Comparison of SO_2 Oxidation Rates Calculated in This Study
to Values Previously Reported for Trajectives in the Los Angeles Basin at That Time of Year

Time of Arrival at Trajectory End Point PDT	July 22, 1977 Ending at Lennox (This Study) k %/hr	July 10, 1973 Ending at Pasadena (Roberts, 1975) k %/hr	July 25, 1973 Ending at Pasadena (Roberts, 1975) k %/hr	July 26, 1973 Ending at Pasadena (Roberts, 1975) k %/hr
800				
900	1.4			
1000				
1100	6.3			5.2
1200		1.2		5.1
1300	10.0	3.0	12.1	8.1
1400		10.0	8.6	4.6
1500	14.0	14.6	10.3	
1600				
1700	6.9			
1800				
1900	2.7			
2000				
2100	0.8			
2200				
2300	4.6			
Average Value	5.8	7.2	10.3	5.8

present study are in the same range as those of Roberts (1975), but with a somewhat lower average value. Considerable scatter in oxidation rate estimates is apparent in both sets of experiments, even for air parcels with consecutive times of arrival at the monitoring sites of interest. This may be due in part to a diurnal variation in SO_2 oxidation rate, but another likely explanation lies in the nature of the experimental conditions encountered in these field studies. Fairly small changes in measured SO_2 or sulfate concentrations can lead to correspondingly larger percentage changes in reaction rate estimates. For example, a 20% reduction in sulfate concentration observed at Lennox between 1400 and 1600 hours on July 22 would have reduced the estimated SO_2 oxidation rate from 14% per hour down to 7.8% per hour. Our calculation scheme further forces agreement between calculated and measured total sulfur oxides concentrations, with the result that the discreteness of the SO_2 concentration measurements (reported only in increments of 0.01 ppm) contributes to scatter in the SO_2 oxidation rate estimates.

In a situation where fluctuations within the limits of experimental error are magnified in their effect on calculated SO_2 oxidation rates, it is probably wise to rely on the average of all eight of our determinations as the best indication of the rate at which sulfates were being formed on this occasion. This overall average SO_2 oxidation rate (as shown in Table 7) was 5.8% per hour. That value compares favorably to the average Los Angeles summertime SO_2 oxidation of 6% per hour estimated from the sulfate air quality model validation study by Cass (1978).

Total sulfur oxides concentrations observed at Lennox on July 22 are shown in Figure 6. On a twenty-four hour average basis, contributors to that pollutant loading included:

- 60% fresh emissions from nearby sources
- 33% backwash sulfur oxides recirculated from over the urban area by the land breeze/sea breeze reversal
- 4% marine sulfur oxides
- 3% overnight emissions tagged with SF_6.

The dominant contribution from fresh emissions is to be expected because Lennox was directly in the path of the plumes from El Segundo point sources during most of the sea breeze portion of July 22.

While total sulfur oxides air quality was dominated by fresh emissions from nearby sources, sulfate concentrations were due largely to the oldest material in the atmosphere. Measurements at Lennox on July 22 yielded a twenty-four hour average sulfate concentration of 32.3 $\mu gm/m^3$. Figure 7 shows that that twenty-four hour average consisted of:

- 49% backwash material
- 20% marine material
- 20% fresh emissions
- 11% overnight emissions tagged with SF_6.

One reason for the relatively modest impact of fresh emissions on Lennox sulfate air quality is found in the initial chemical composition of those fresh SO_x emissions. Nearly all of the fresh SO_x emissions are evolved from their source as SO_2. In the late morning and early

Figure 6

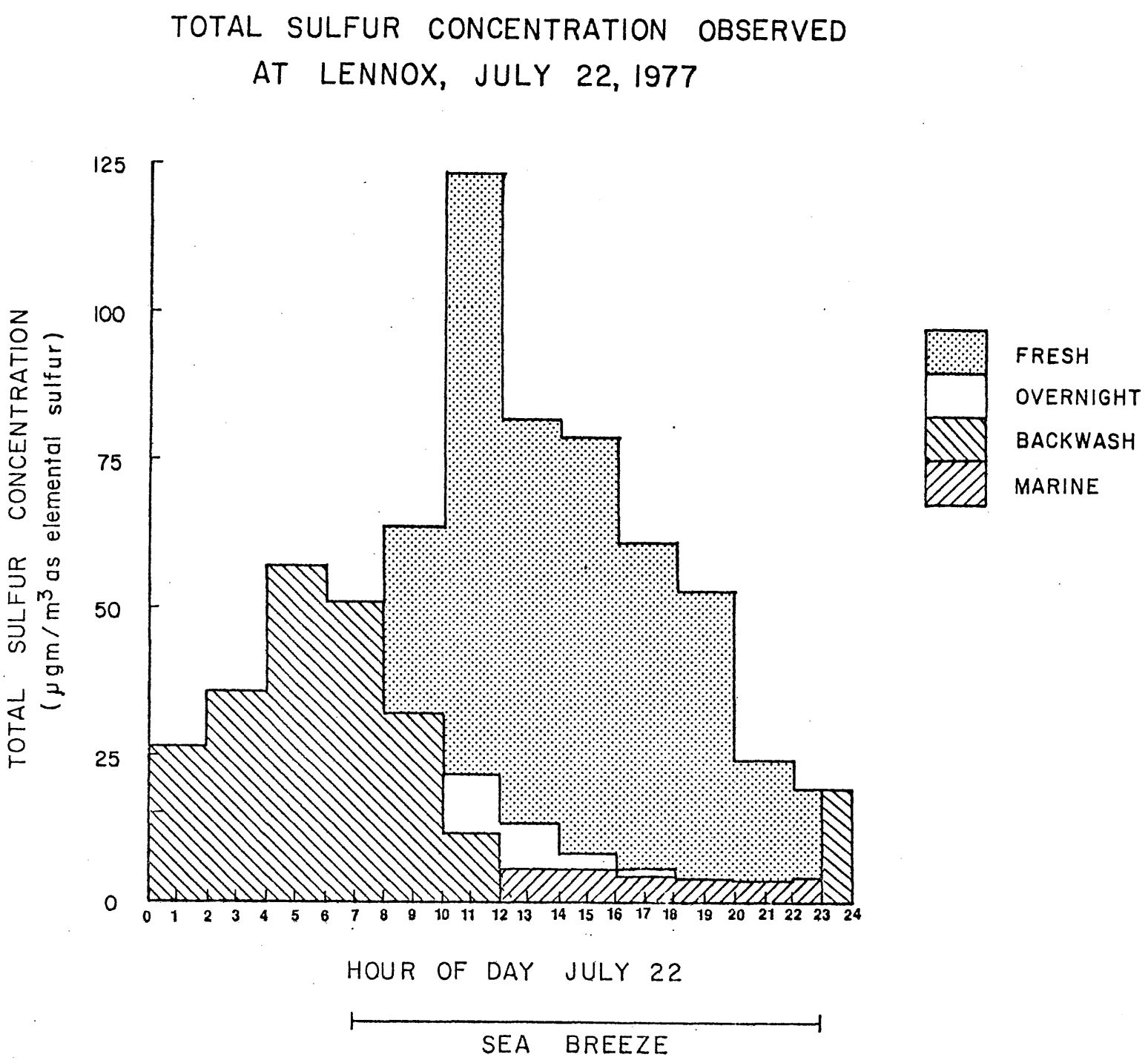
TOTAL SULFUR CONCENTRATION OBSERVED
AT LENNOX, JULY 22, 1977
TOTAL SULFUR CONCENTRATION
(μgm/m³ as elemental sulfur)
125
100
75
50
25
0
0 1 2 3 4 5 6 7 8 9 10 11 12 13 14 15 16 17 18 19 20 21 22 23 24
HOUR OF DAY JULY 22
SEA BREEZE
FRESH
OVERNIGHT
BACKWASH
MARINE

Figure 7

SULFATE CONCENTRATIONS OBSERVED AT LENNOX
JULY 22, 1977

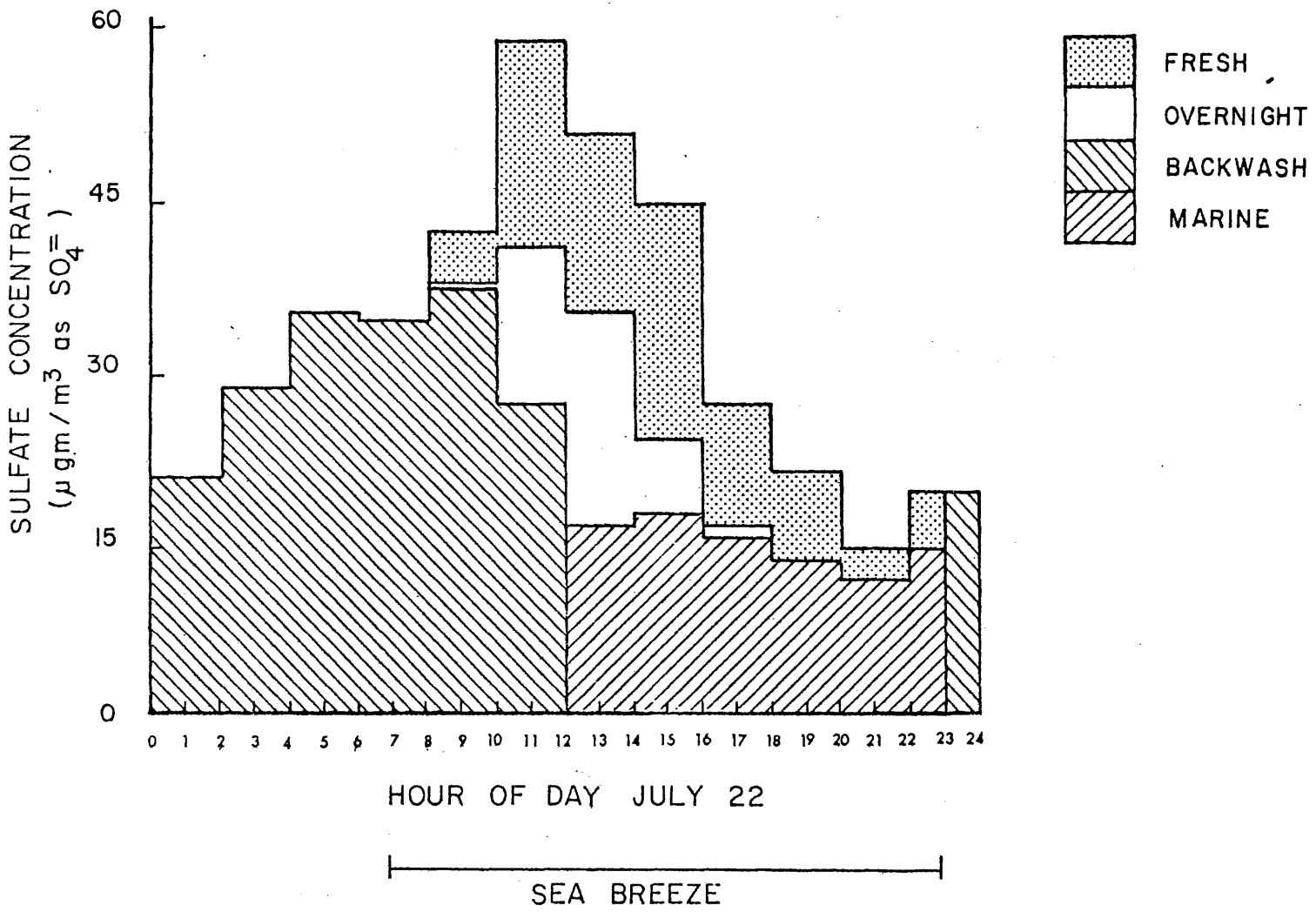

afternoon of July 22, transport times from El Segundo to Lennox were less than one hour. Sulfate formation was slow enough that fresh SO_x emissions still existed predominantly as SO_2 at the time that they crossed the Lennox monitoring site. In contrast, backwash and marine air parcels carried a significant fraction of their total sulfur oxides concentrations as sulfates at the time of their initial characterization. Over long retention times, additional sulfates formed by oxidation of SO_2, while total sulfur in marine and backwash air parcels declined due to surface deposition of SO_2. The result is that these aged air masses were major contributors to observed sulfate concentrations in spite of their reduced importance to total sulfur oxides concentrations. The sea breeze/land breeze circulation system made possible the long retention times needed for sulfate accumulation in backwash air parcels.

A second effect of the sea breeze/land breeze circulation system is to increase sulfate concentrations due to multiple passes of the same air mass over the same emission sources. This feature is most clearly illustrated by considering the peak sulfate concentrations which occurred at Lennox between 1000 and 1200 hours on July 22. The air mass passing Lennox during that time interval contained neither the highest backwash contribution observed, nor the highest overnight or fresh emissions impacts observed over a two hour period. The superposition of pollutant contributions from several distinct passes of the same air mass over coastal point sources, however, was sufficient to accumulate the high concentrations observed at that time.

REFERENCES

Cass, G. R. (1978), Methods for Sulfate Air Quality Management with Applications to Los Angeles, PhD Thesis, California Institute of Technology.

Davidson, C. I. (1977), Deposition of Trace Metal-Containing Aerosols on Smooth, Flat Surfaces and on Wild Oat Grass, PhD Thesis, California Institute of Technology (see Appendix II).

Garland, J. A. (1974), "Dry Deposition of SO_2 and Other Gases", in Atmosphere-Surface Exchange of Particulate and Gaseous Pollutants (1974), R. J. Engelmann and G. A. Sehmel, editors, Technical Information Center, Office of Public Affairs, U.S. Energy Research and Development Administration, 1976.

Hunter, S. C. and N. L. Helgeson (1976), Control of Oxides of Sulfur from Stationary Sources in the South Coast Air Basin of California, Tustin, California, KVB Incorporated, Document Number KVB 5802-432, prepared under California Air Resources Board Contract Number ARB 4-421.

McCullough, G. (1978), Los Angeles Department of Water and Power, personal communication.

Roberts, P. T. (1975), Gas-to-Particle Conversion: Sulfur Dioxide in a Photochemically Reactive System, PhD Thesis, California Institute of Technology.

Tsou, G. et al. (1977), "Sulfate Data at Lennox, Redondo Beach, and Santa Catalina Island in July 1977", El Monte, California, California Air Resources Board, Aerosol Laboratory staff report.

Chapter 4

TRANSPORT OF SULFUR OXIDES WITHIN THE LOS ANGELES SEA BREEZE/LAND BREEZE CIRCULATION SYSTEM

by

Glen R. Cass
Environmental Engineering Science Department
and
Environmental Quality Laboratory
California Institute of Technology

and

Fredrick H. Shair
Division of Chemistry and Chemical Engineering
California Institute of Technology
Pasadena, California 91125

March 1980

Reprinted from the Volume of Conference Papers: Second Joint Conference on Applications of Air Pollution Meteorology and Second Conference on Industrial Meteorology, 24-28 March 1980, New Orleans, La. Published by the American Meteorological Society, Boston, Mass.

5.3

Reprinted from the Volume of Conference Papers: Second Joint Conference on Applications of Air Pollution Meteorology and Second Conference on Industrial Meteorology, 24-28 March 1980, New Orleans, La. Published by the American Meteorological Society, Boston, Mass.

TRANSPORT OF SULFUR OXIDES WITHIN THE LOS ANGELES SEA BREEZE/LAND BREEZE CIRCULATION SYSTEM

Glen R. Cass

Environmental Engineering Science Department
and
Environmental Quality Laboratory
California Institute of Technology

Fredrick H. Shair

Chemical Engineering Department
California Institute of Technology
Pasadena, California 91125

1. INTRODUCTION

The sea breeze/land breeze circulation system in the Los Angeles area results in transport of pollutants seaward at night followed by return of aged material inland the next day. This characteristic wind reversal pattern both increases the retention time available for the oxidation of SO_2 to form sulfates and causes individual air parcels to make multiple passes over large coastal emissions sources. As a result, the Los Angeles atmosphere exhibits high peak day and high annual mean sulfate concentrations in spite of the fact that sulfate concentrations in marine background or desert air are low.

The problem of identifying the impact of individual emissions sources on sulfate air quality in such a situation is so complicated that it will frustrate many conventional air quality modeling approaches. Transport and chemical reaction processes must be followed for several consecutive days within an airmass that "sloshes" back and forth over thousands of emissions sources. Unsteady meteorological conditions characterized by light and variable winds render Gaussian plume calculations inappropriate. The large spatial domain needed to confine several days' emissions, combined with the absence of meteorological data over the ocean make even finite difference scheme grid-based air quality models unattractive.

However, over the past five years a series of research projects have shown how SF_6 tracer studies combined with chemical modeling can be used to verify the origin of the high sulfate levels observed in Los Angeles. Transport patterns, dispersion rates and SO_2 oxidation rates have been measured during SF_6 tracer experiments. Emissions to air quality models have been constructed and validated using data from the tracer studies. Source contributions to observed sulfate air quality have been separated into the impact of distinctly different types of emissions sources. Emissions control strategies aimed at sulfate air quality improvement have been designed.

The purpose of this paper is to review and integrate the findings of research projects at Caltech which bear on the resolution of the Los Angeles sulfate air quality problem.

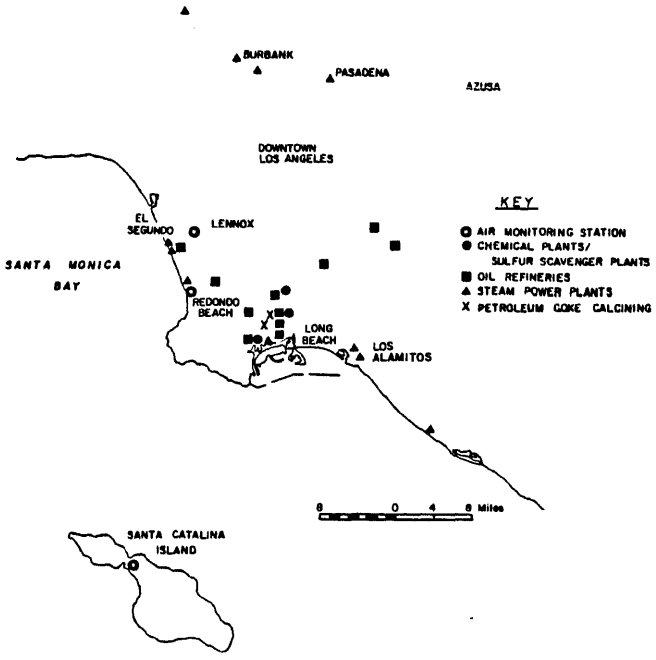

Figure 1. Major Sources of Sulfur Oxides Emissions in the Los Angeles Area.

The original reports on each individual project are cited and are available elsewhere.

2. SULFUR OXIDES EMISSIONS

The location of interest is the Southern California coastline of meteropolitan Los Angeles and Orange Counties, as shown in Figure 1. The major sources of sulfur oxides emissions are located along the coast, close to waterborne transportation and a supply of cooling water.

Emissions from these sources during each month of the years 1972 through 1974 are shown in time series in Figure 2. An underlying contribution to sulfur oxides emissions from mobile sources is shown which exhibits only slight seasonal variation. To that is added a contribution from miscellaneous stationary sources, primarily from petroleum coke calcining kilns. The petroleum refinery emissions shown arise principally from refinery fluid catalytic cracking units. The

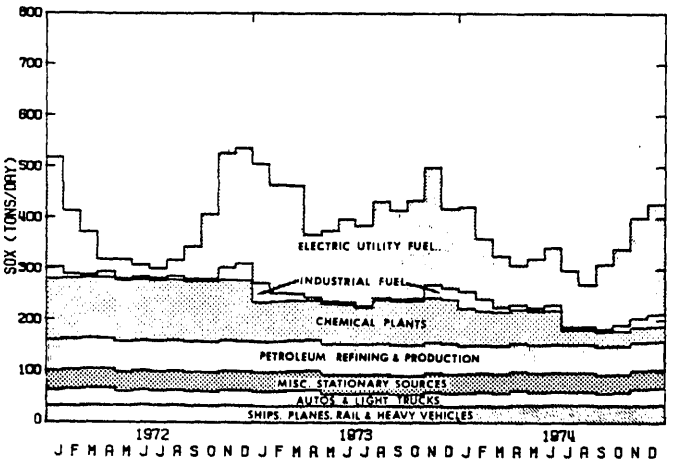

Figure 2. Sulfur Oxides Emissions within the Geographic Area Shown in Figure 1. (from Cass, 1978)

chemical plant emissions arise from sulfur recovery and sulfuric acid plants which reclaim by-products from refinery wastes. A strong seasonal variation in power plant and industrial fuel burning SO_x emissions is evident as interruptible natural gas customers switch to fuel oil in the winter months in order to free natural gas supplies for home heating use. Of particular interest to this study are the two groups of large power plants located at El Segundo and at Los Alamitos (see Fig. 1) which will be the subject of SF_6 tracer releases.

3. LOS ANGELES SULFATE AIR QUALITY

Historical routine air monitoring data for sulfates and SO_2 were assembled and reviewed by Cass (1975; 1978). It was found that SO_2 concentrations in Los Angeles dropped rapidly with distance inland from major coastal point sources, as would be expected for dispersion of a conserved or slowly decaying pollutant species. In contrast, sulfate concentrations throughout the entire Los Angeles Basin averaged between 10 and 14 $\mu gm/m^3$ over long periods of time, and were as high in the immediate vicinity of major sulfur oxides sources as in the far inland valleys (see Figure 3). Long distance transport of pollutants from other airsheds could not account for this behavior since air quality measurements at islands off the southern California coast and in desert areas surrounding Los Angeles all showed much lower sulfate concentrations, in the range 3 to 5 $\mu gm/m^3$, annual mean.

Two hypotheses were offered which might explain the observed spatial distribution of sulfate air quality (Cass, 1975). During periods of direct inland transport from source to receptors, the constant sulfate concentration with distance inland from the coast could be explained by a competition between dispersion which tends to lower pollutant concentrations and additional gas-to-particle conversion involving SO_2 which tends to build-up sulfate concentrations. An alternative possibility is that sulfate concentrations accumulate aloft near the coast during late night land breeze and early morning stagnation periods. This well-aged aerosol might then be swept across the basin the next day by the advancing

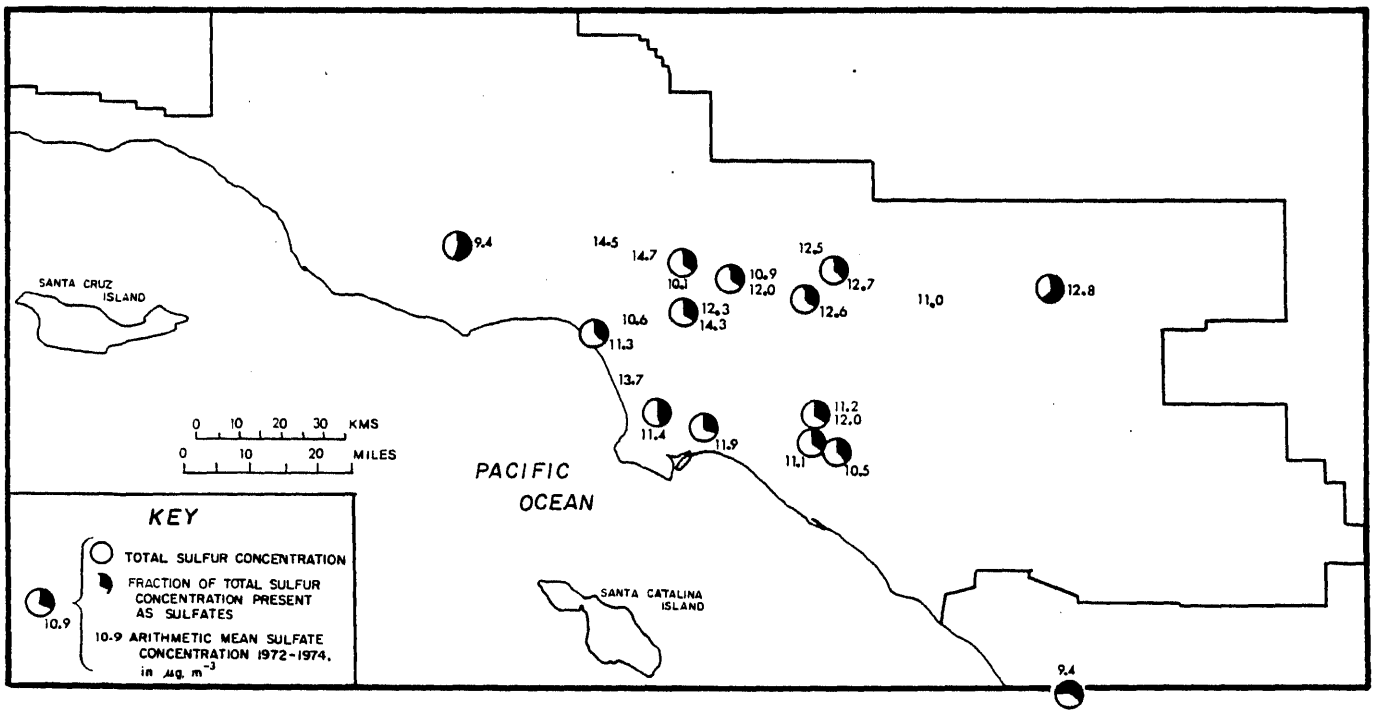

Figure 3. Arithmetic Mean Sulfate Air Quality: 1972 through 1974 Concentrations Shown Adjacent to Monitoring Site Location in $\mu gm/m^3$ (from Cass, 1978).

sea breeze, contributing roughly equal amounts of sulfate to successive air monitoring stations in passing.

SF_6 tracer studies were designed to probe each of these transport patterns.

4. DIRECT INLAND TRANSPORT

Under fully developed sea breeze conditions, direct transport occurs from coastal sources to inland areas of the Los Angeles basin. In order to determine both the path of those plumes and the rate of their crosswind dispersion, two series of SF_6 tracer experiments were conducted.

During October and November, 1974 a total of six SF_6 tracer releases were made from stacks at the two power plants located at Los Alamitos, as shown in Figure 1 (Drivas and Shair, 1975). Three of these tests were conducted at the Los Angeles Department of Water and Power Haynes Plant, and the other three releases were made from a stack at the Southern California Edison Company Alamitos Generating Station. The two stacks were only 400 m apart and are indicated by a single release point (⊠) on the map of Figure 4. SF_6 was injected at a rate of between 4.83 and 8.97 g/sec into the power plants stack gases in order to achieve an SF_6 concentration in the stack of between 2.00 and 2.63 ppm.

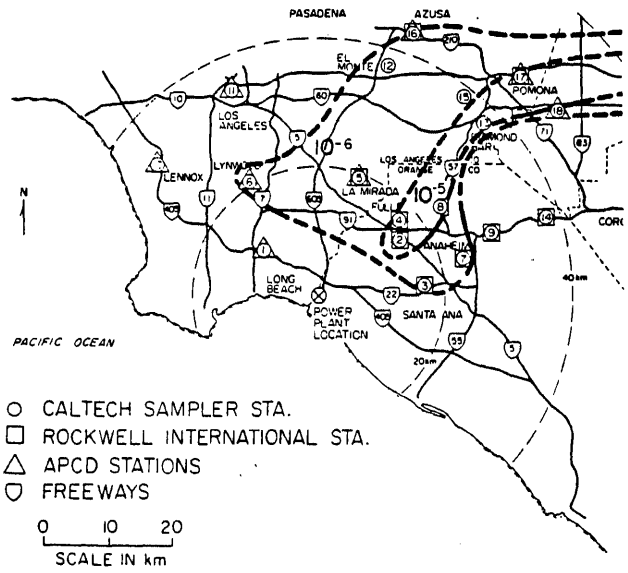

Figure 4. Three-Hour Averaged Concentration Isopleths for Power Plant Test No. 2: 2 pm to 5 pm (PST) October 11, 1974. Isopleths show degree of dilution relative to stack concentration (from Drivas and Shair, 1975).

Twenty-two fixed ground level SF_6 monitoring sites plus ground level automotive traverses across the path of the power plant plumes were used to map the location of the plumes. The crosswind standard deviation of plume spread as a function of travel time downwind over the Los Angeles urban area was computed. A typical plume map, shown in Figure 4, indicates that the plumes are present at ground level about 10 miles from the power plants and proceed in a narrow arc toward the northeast passing through Pomona. The plumes then typically turn eastward at the base of the high mountains which ring the back of the Los Angeles Basin and travel east through San Bernardino. This transport pattern was observed during all or part of each of the six tests conducted.

A second set of sea breeze tracer studies was conducted by Shair et al. (1980) during September 1977. SF_6 was released from a ship stationed offshore in the Santa Monica Bay and was followed to a downwind distance of 88 km. Again a network of ground-based monitoring sites plus automobile traverses across the plume were used to map its location and to calculate the crosswind standard deviation of plume spread.

Data on the crosswind dispersion of plumes over continuous urban areas are rare. Perhaps the best known and most often used results are those due to McElroy and Pooler (1968). In that study, dispersion over the St. Louis urban area was tracked out to a travel time of about 4×10^3 sec (66.7 min) downwind. Data from the Los Angeles SF_6 tracer studies were assembled and analyzed by Cass (1978). It was possible to show that the Los Angeles data fall within the extrapolated bounds of the dispersion observed during McElroy and Pooler's most stable and least stable atmospheric conditions. The Los Angeles data however span travel times up to 26.1×10^3 sec (435 min). In this manner, our ability to verify dispersion rates over urban areas was extended to time scales long enough to be important to a study of sulfate formation in the atmosphere.

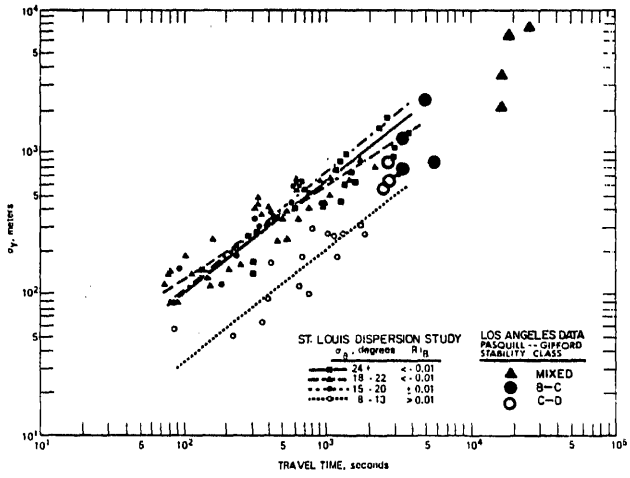

Figure 5. Crosswind standard deviation of tracer material as a function of travel time in terms of standard deviation of wind direction fluctuations (σ_θ) and bulk Richardson number (Ri_B), from McElroy and Pooler (1968), plus Los Angeles data from Drivas and Shair (1975) and Shair et al. (1980). Data reduced by Cass (1978).

5. SULFATE FORMATION IN THE SEA BREEZE/ LAND BREEZE CIRCULATION SYSTEM

Having verified the transport patterns and dispersion rates which occur under conditions when plumes are transported directly inland, attention was turned to the second flow regime of interest. Could it be shown that sulfur oxides air pollutants sent seaward at night by the land breeze were being returned inland the next day after having aged overnight in the marine environment?

A study of surface wind trajectories was conducted by Lyons (1975) to estimate the liklihood that pollutants sent seaward at night would return back across the Los Angeles County coast the next day. It was found, for example, that for a release at the surface into a land breeze at Redondo Beach in September or October 1973, there was an 89% probability that the tracer would be detected recrossing the coast within 19 hours after a 2:00 am release.

A series of field tests then were designed to confirm that pollutant recirculation also occurs for the case of elevated releases from large power plants (Shair et al. 1980). On July 22, 1977 SF_6 was released into the land breeze from a stack at the Southern California Edison Company El Segundo Generating Station. A total of 90 kg of SF_6 was discharged beginning at 00:00 hours Pacific Daylight Time on July 22 and ending at 05:00 hours on the morning of that day. SF_6 monitors were located aboard a ship traveling back and forth across Santa Monica Bay. The ship borne data showed that that power plant plume stayed aloft until about 5:30 am, after which fumigation to the ocean's surface occurred within a few minutes over a wide area of Santa Monica Bay.

Trajectories calculated from surface winds indicated that the emissions sent seaward tacked northward before recrossing the coastline the next morning. A line of closely spaced SF_6 monitors located at the coast however showed non-zero SF_6 concentrations returning inland from Ventura County south to Redondo Beach. Mass balance calculations performed on the SF_6 as it recrossed the line of coastal samplers showed that virtually 100% of the tracer could be accounted for, as shown in Figure 6. The peak returning SF_6 concentration recrossed the coast at the El Segundo monitoring site between 10:00 and 11:00 hours the next day. The point of highest pollutant impact thus crossed the coast the next morning near the point of pollutant origin. As it passed over the power plants and refinery complex at El Segundo for the second time, that air parcel would have received a second dose of pollutant emissions before beginning its journey across the Los Angeles Basin transported by the day's sea breeze.

A sulfate air quality monitoring station was established during this test at Lennox, which is located just inland from the El Segundo SF_6 release point. A second onshore sulfate monitoring station was set-up at Redondo Beach and a marine background site was established at Santa Catalina Island (Tsou et al., 1977). Data on SO_2 concentrations at Lennox and Redondo Beach are available from monitoring instruments operated by the South Coast Air Quality Management District.

Chemical reaction and ground level deposition calculations then were performed along the path of pollutant transport in order to determine the origin of pollutants contributing to the sulfate loading observed at Lennox (Cass and Shair, 1978). Urban backwash air parcels were defined as that material stored inland at the end of the prior day's sea breeze that was transported back to sea by the nighttime land breeze. These pollutants were tracked by means of surface wind trajectories.

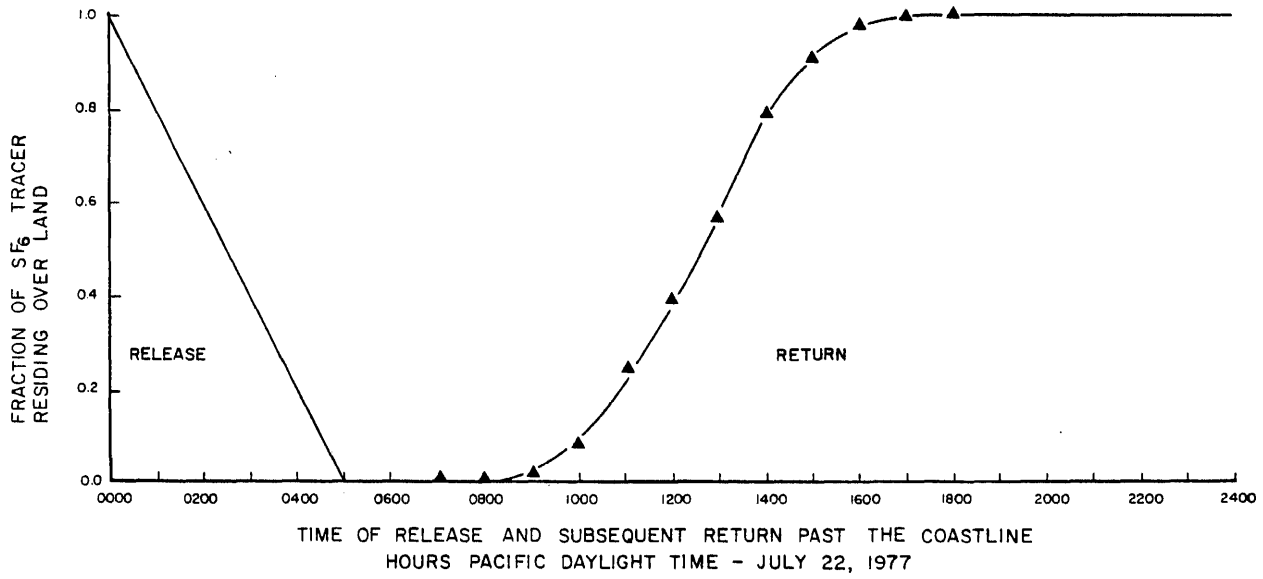

Figure 6. SF_6 Tracer Cumulative Release and Return From Emissions at El Segundo Power Plant into Nighttime Land Breeze Regime (from Cass and Shair, 1978).

Overnight emissions from the El Segundo area were identified by means of the SF_6 tracer. The intrusion of marine air uncontaminated by local emissions sources was identified by trajectory calculations and by reference to the Santa Catalina Island monitoring station. The presence at Lennox of fresh emissions released in the morning following the 5:00 am end of the tracer experiment were detected on the basis of sulfur balances on sulfate and total sulfur concentrations measured at Lennox. For the method of performing these air quality modeling calculations, see Cass and Shair (1978).

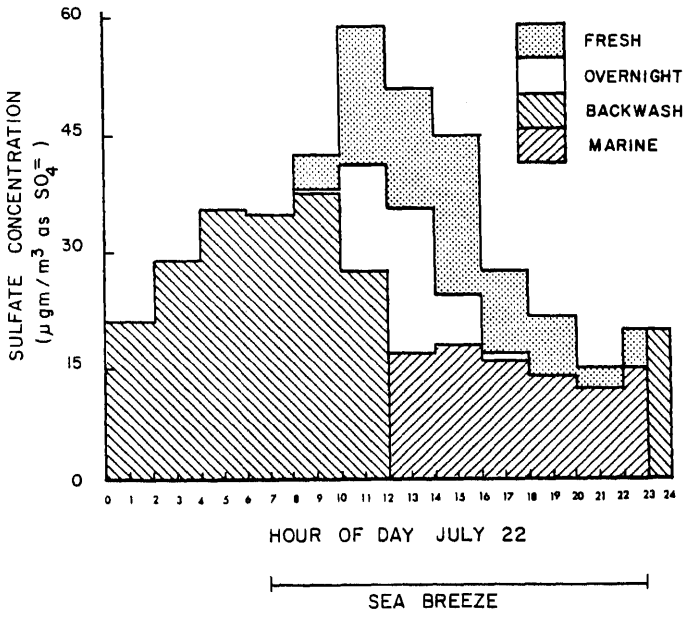

Figure 7. The Origin of Sulfate Concentrations Observed at Lennox July 22, 1977. (from Cass and Shair, 1978)

It was found that the total sulfur oxides concentrations observed that day at Lennox, California were dominated by freshly emitted SO_2 from nearby sources. In contrast, sulfate concentrations observed were due largely to the oldest material in the atmosphere. Measurements at Lennox on July 22 yielded a 24 hour average sulfate concentration of 32.3 $\mu gm/m^3$ which as shown in Figure 7 consisted of:

- 49% sulfates held over from the previous day ("Backwash" recirculated by the land breeze/sea breeze reversal)
- 20% sulfates of marine background origin
- 20% sulfates from "fresh" emissions which occurred in the late morning and afternoon near the sampling site
- 11% sulfates from "overnight" emissions into the land breeze between midnight and the onset of the early morning sea breeze (tagged with SF_6).

The overall rate of SO_2 oxidation to form sulfates in the Los Angeles atmosphere was estimated to average about 5.8% per hour during these experiments.

6. SULFATE AIR QUALITY CONTROL STRATEGY DESIGN

An emissions control strategy study was conducted by Cass (1978) to assess the least costly means for reducing the ambient sulfate concentrations in the Los Angeles atmosphere. An important part of that study involved the construction and validation of a spatially and temporally resolved regional air quality model which relates sulfur oxides emissions to long-term average sulfate air quality. The SF_6 tracer studies played an important role in the model validation process by confirming parameter estimates for dispersion rates, SO_2 oxidation rates, and by providing a check on typical transport patterns.

The air quality simulation model developed computes pollutant concentrations from long-run average source to receptor transport and reaction probabilities. These transport and reaction probabilities in turn were estimated from Lagrangian marked particle statistics based on the time sequence of historical measured wind speed, wind direction, and inversion base height motion within the airshed of interest. First order chemical reactions and pollutant dry deposition were incorporated. The model was adapted to a multiple source urban setting in a way which permits retention of the air quality impact of each source class contributing to air quality predictions at each receptor site.

The calculation procedure used in that air quality model has been summarized briefly as follows. Single particles marked with the magnitude and initial chemical composition of sulfur oxides emissions from each source are inserted at measured time intervals into the atmosphere above the location of their points of origin. Depending on the plume rise characteristics of each source and meteorological conditions at the time of release, a pollutant parcel may be inserted either above or below the base of the temperature inversion which separates a well mixed layer next to the ground from a stable air mass aloft.

As these sulfur oxides laden air parcels are transported downwind, chemical reactions and surface removal processes act to alter the mass of SO_2 and sulfates represented by each particle. Sulfur oxides residing within the mixed layer next to the ground are affected both by ground level dry deposition and by atmospheric oxidation of SO_2 to form additional sulfates. Pollutant parcels stored within the stable layer aloft are isolated from surface removal processes but still are available for chemical reaction. Exchange of air parcels between the mixed layer next to the ground and the stable layer aloft occurs as inversion basing height changes over time.

The trajectories of successive particles released from a source form streaklines downwind from that source. Streaklines present at each hour of the month are computed and superimposed. The horizontal displacement of each particle located below the inversion base is paired with the particle's probable chemical status and divided by the depth of the mixed layer at the time that the streakline of interest was computed. The resulting magnitudes are assigned to a matrix of

receptor cells by summing the contribution for all particles falling within the same receptor cell. Totals are accumulated separately for SO_2 and for sulfates. The accumulated totals are divided by the dimensions of a receptor cell and the number of time steps being superimposed in order to directly obtain the spatial distribution of long-term average SO_2 and sulfate concentrations appearing throughout the airshed.

By repeating that process for each source in the airshed and superimposing the results onto an estimate of sulfate background air quality, a multiple source urban air quality model for sulfates is obtained. Superposition is permitted because all chemical processes are modeled in a form that is linear in emissions.

A grid system consisting of 2 mile by 2 mile squares was laid down over the geographic area shown in Figure 1. Emissions sources falling within each grid square were identified and separated into 26 classes of mobile and stationary sources within the 7 broad categories outlined in Figure 2. Each emissions source class was composed of a group of like equipment (e.g. sulfuric acid plants) that would be subject to compliance with a common emission control regulation.

The air quality model next was tested in Los Angeles over each month of the years 1972 through 1974. As shown in Figures 8 and 9, good agreement was obtained between computed and historically observed sulfate concentrations. Summertime SO_2 oxidation rates averaging 6% per hour were computed during the air quality modeling study, in

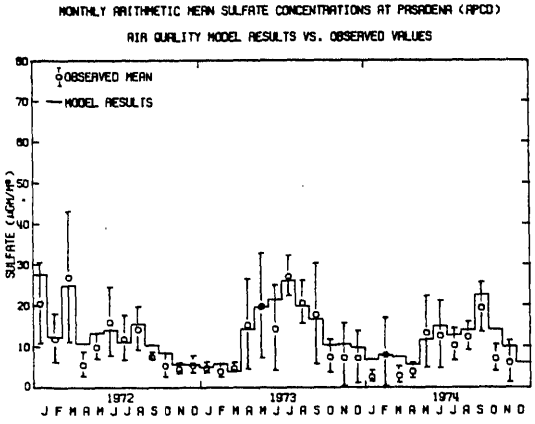

Figure 8. (from Cass, 1978)

good agreement with the results of the SF_6 tracer analysis described previously. A seasonal variation in SO_2 oxidation rate was inferred from air quality model calculations, with wintertime SO_2 oxidation rates declining to between 0.5% and 3.0% per hour. Transport paths downwind of the Los Alamitos power plants computed during periods of direct inland transport are shown in Figure 10 and may be compared to the SF_6 tracer study results of Figure 4.

All source class contributions to sulfate air quality computed from the air quality model are superimposed and averaged over the year 1974 in Figure 11. It is seen that the sulfate concentrations predicted in near coastal locations

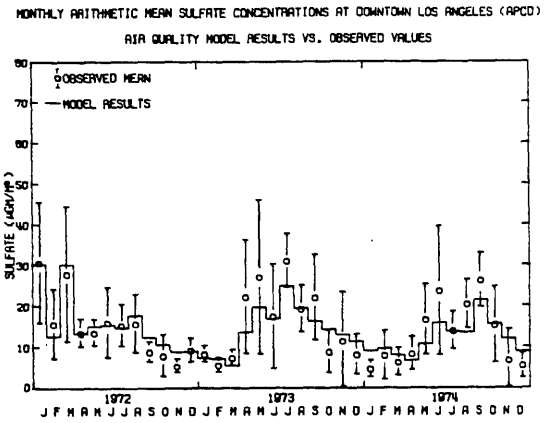

Figure 9. (from Cass, 1978)

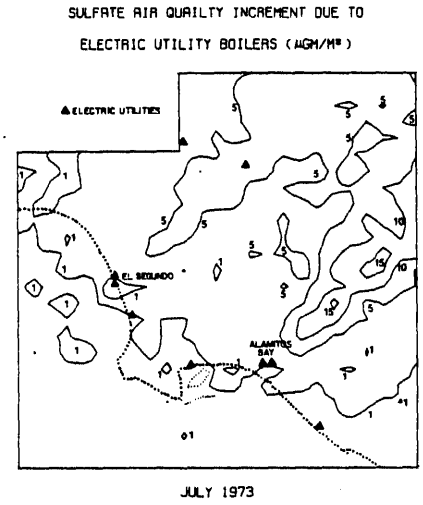

Figure 10. (from Cass, 1978)

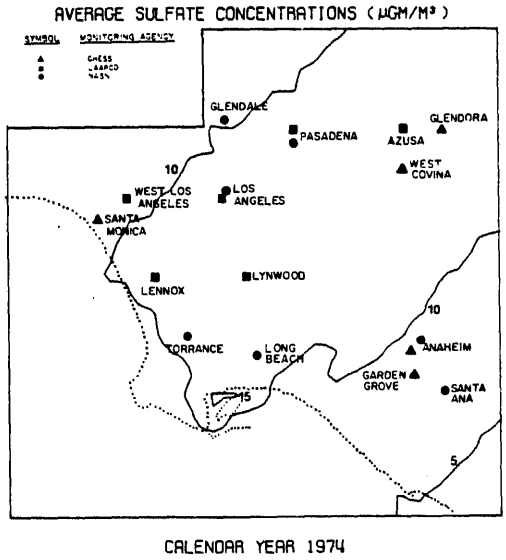

Figure 11. (from Cass, 1978)

are of the same magnitude as those computed far downwind, as must be the case if the air quality data of Figure 3 are to be closely reproduced.

In winter months with a pronounced daily sea breeze/land breeze wind reversal, air parcel trajectories wander widely over the basin. Sulfur oxides emitted from all source classes are dispersed widely within the airshed by the rotation of the wind vectors. In contrast, during mid-summer, onshore flow persists for most of the day. However, the sequential siting of major SO_x sources along the coast means that the central portion of the air basin is downwind of one major source group or another at most times. Lateral dispersion of emissions is just about sufficient to balance sulfate formation, with the result that upwind/downwind pollutant gradients are rather small in spite of the direct inland transport from sources to receptors. Annual mean sulfate concentrations are further smoothed by seasonal transport cycles in which peak sulfate concentrations appeared far inland during the summer and near the coast during the winter.

Source class contributions to observed sulfate air quality are shown in Figures 12 and 13. Superposition of small pollutant increments from power plants, heavy duty mobile sources, chemical plants, refineries and other sources, plus background sulfates must be considered in order to come close to explaining observed pollutant concentrations. Since no single type of emissions source dominates local sulfate air quality, a

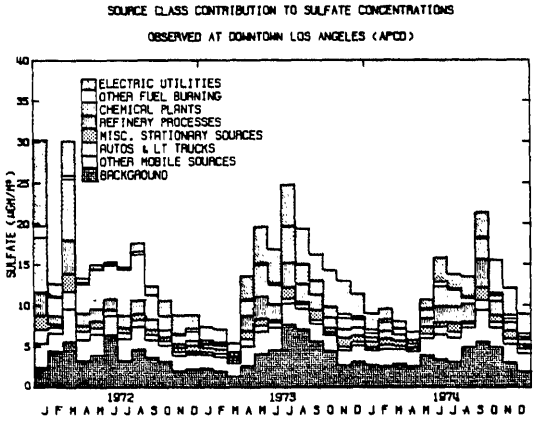

Figure 12. (from Cass, 1978)

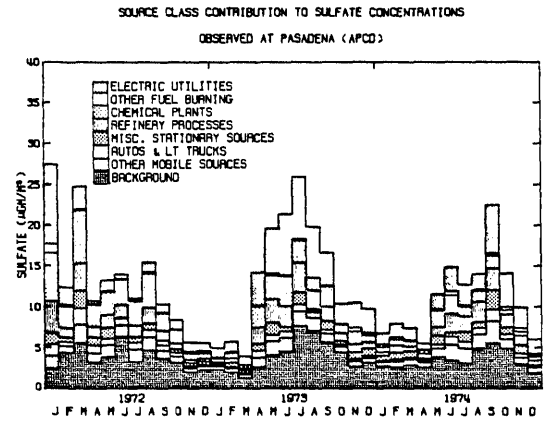

Figure 13. (from Cass, 1978)

control program diversified over a large number of emissions source types will be needed if a significant improvement in sulfate air quality is sought in the Los Angeles region. One such emission control strategy identified by Cass (1978) is shown in Figure 14, organized in order of increasing marginal cost per unit of sulfate concentration reduction.

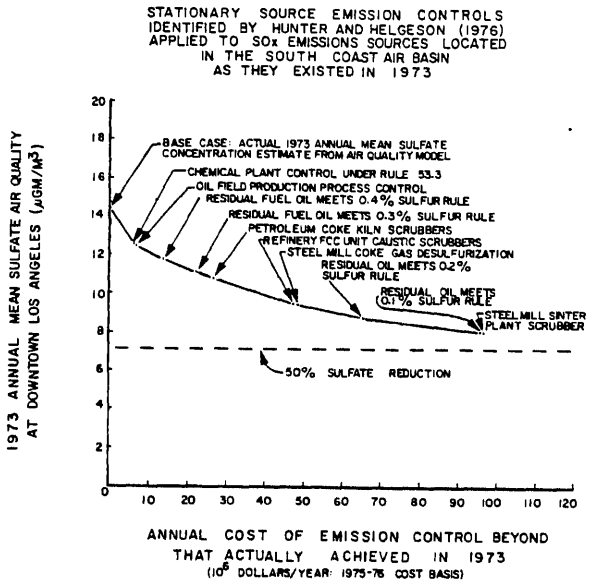

Figure 14. (from Cass, 1978)

7. CONCLUSIONS

The combination of SF_6 tracer studies and air quality modeling has been used to examine the transport and reaction of sulfur oxides air pollutants in the Los Angeles area atmosphere. The tracer studies provide an attractive means for obtaining data for air quality model validation studies involving very complex meteorological conditions.

The the course of these studies, several important hypotheses about the origin of the Los Angeles sulfate problem have been tested and confirmed. The sea breeze/land breeze circulation system in Los Angeles causes an increase in retention time for sulfate formation in this airshed. Pollutants held over from the previous day and pollutants emitted at night can be transported seaward on the land breeze, only to return many hours later as the sea breeze reversal in wind direction occurs. Both SF_6 tracer studies of single episodes and long-term air quality modeling studies indicate a summertime SO_2 oxidation rate which averages about 6% per hour.

Information gained from these studies holds important implications for emissions control strategies aimed at sulfate air quality improvement. From Figure 7 it is seen that peak sulfate concentrations near the coast can be caused by multiple passes of the same airmass over coastal point sources. This recirculation is induced by the sea breeze/land breeze system. Intermittent control strategies aimed at reducing sulfate concentrations by switching fuel at major sources on the same day as an episode forecast will achieve only limited

results. This is because so much of the material contributing to that day's sulfate concentrations is either held over from the previous day and night, or is due to long distance transport of regional background through the marine environment. If large sulfate concentration reductions are sought, it will probably be necessary to place continuous controls on emissions sources in order to prevent the build-up of sulfates on days preceeding the worst episodes. Air quality control strategy studies described in this paper have shown how emissions to air quality models can be used to identify combinations of emissions controls on a wide variety of sources that could cut long-term average sulfate concentrations in Los Angeles by about 50%.

Acknowledgment

This work reviews research sponsored by the California Air Resources Board under contracts numbered ARB-3-915, ARB-A6-061-87 and ARB-A6-202-30. The authors are happy to acknowledge the interest and help given to them by Charles Bennett and Jack Suder.

REFERENCES

Cass, G.R. (1975) "Dimensions of the Los Angeles SO_2/Sulfate Problem," Pasadena, California, California Institute of Technology, Environmental Quality Laboratory Memorandum 15.

Cass, G.R. (1978) Methods for Sulfate Air Quality Management with Applications to Los Angeles, Ph.D. Thesis, California Institute of Technology. Available from University Microfilms, Ann Arbor, Michigan.

Cass, G.R. and Shair, F.H. (1978) "Sulfate Accumulation in the Los Angeles Sea Breeze/Land Breeze Circulation System," California Institute of Technology, draft report submitted to the California Air Resources Board under Contract ARB-A6-202-30.

Drivas, P.J. and Shair, F.H. (1975) The Chemistry, Dispersion, and Transport of Air Pollutants Emitted from Fossil Fuel Power Plants in California--Transport and Dispersion of Plumes Associated with the Complex Coastal Meteorology. Division of Chemistry and Chemical Engineering, California Institute of Technology. Final Report to the California Air Resources Board under Contract ARB-3-915. Available from NTIS.

Lyons, C.E. (1975) "The Proposal and Preparation of a Field Study Using Gaseous Tracers to Examine the Impact of the Diurnal Coastal Wind Cycle on the Dispersion of Pollutants over the Los Angeles Basin," Report submitted as part of completion of the requirements for the degree of Master of Science in Chemical Engineering, California Institute of Technology.

McElroy, J.L. and Pooler, F. Jr. (1968) "St. Louis Dispersion Study, Volume II--Analysis," Arlington, Virginia, U.S. Public Health Service, National Air Pollution Control Administration Publication No. AP-53.

Shair, F.H. et al. (1980) "Application of Atmospheric Tracer Techniques to Determine the Transport and Dispersion Associated with the Land Breeze-Sea Breeze Movement of Air over the Los Angeles Coastal Zone," California Institute of Technology, Final Report to the California Air Resources Board under Contract ARB-A6-202-30 (in preparation).

Tsou, G. et al. (1977) "Sulfate Data at Lennox, Redondo Beach, and Santa Catalina Island in July 1977," El Monte, California Air Resources Board, Aerosol Laboratory staff report.

Chapter 5

UNCERTAINTIES ASSOCIATED WITH THE ESTIMATION OF MASS BALANCES AND GAUSSIAN PARAMETERS FROM ATMOSPHERIC TRACER STUDIES

by

Philip A. Sackinger
Danny D. Reible[†]

and

Fredrick H. Shair[††]
Division of Chemistry and Chemical Engineering
California Institute of Technology
Pasadena, California 91125

October 1981

Submitted to Journal of the Air Pollution Control Association

[†]Current address: Department of Chemical Engineering, Louisiana State University, Baton Rouge, Louisiana 70803

[††]To whom correspondence should be addressed

Uncertainties Associated with the Estimation of Mass Balances and Gaussian Parameters from Atmospheric Tracer Studies

by

Philip A. Sackinger
Danny D. Reible[†]
and
Fredrick H. Shair[††]

Division of Chemistry and Chemical Engineering
California Institute of Technology
Pasadena, California 91125

October 1981

[†]Current address: Dept. of Chem. Eng., Louisiana State Univ., Baton Rouge, La. 70803

[††]To whom correspondence should be addressed

ABSTRACT

Data resulting from two atmospheric tracer experiments in the land-sea breeze winds in Los Angeles, California are used to compare the observed and released amounts of tracer (a mass balance). The mass balance calculation indicated that essentially all of the tracer transported to sea during the land breeze was transported back across the shore during the subsequent sea breeze. A methodology for calculating a mass balance and the associated uncertainties is presented. The experimental and calculation procedures presented allowed mass balance estimates with less uncertainty than is present in individual measurements of concentration or mixing height.

Similarly, a methodology for calculating dispersion parameters for the Gaussian plume model from tracer data is discussed and applied to the results of two atmospheric tracer studies conducted during the afternoon sea breeze in the Santa Barbara Channel of California. The method presented involves the integral definitions of the statistical quantities. By considering only tracer concentrations greater than 10% of the maximum concentration, and by considering sufficiently many data points, the uncertainty associated with the parameter estimation was again less than the relative uncertainties in any individual data point.

These studies were primarily designed to relate the uncertainties in estimates of mass balances and in estimations of Gaussian parameters to the uncertainties inherent within field data.

INTRODUCTION

Interest in atmospheric tracer studies has increased greatly during the last few years. Typically the results of such studies have been used to estimate empirical parameters of dispersion models, such as the Gaussian plume model (Turner, 1970)[4]. Also, to ensure the accuracy of the parameter estimation, or to accurately evaluate downwind impact, estimates of mass and/or flux balances are of great help. Unless a major portion of the tracer can be accounted for by means of such balances the associated field study results will be of limited value. The purpose of this paper is to demonstrate through example (1), a technique for estimating nominal values and uncertainties of mass balances incorporating field data and, (2), a technique for estimating nominal values and uncertainties of Gaussian dispersion parameters from field data.

PRESENTATION AND DISCUSSION OF RESULTS

MASS BALANCE ESTIMATES

Until recently, the application of mass balance calculations to atmospheric tracer studies had been limited due to the quality and quantity of available tracer and meterological data. However, the quantity of tracer and meteorological data has increased greatly during recent studies; additionally, the use of gaseous tracers (such as SF_6) has significantly improved the quality of data as compared to particle tracers, when used to tag specific masses of air (Lamb, 1978,[1] Reible, 1982[2]).

Two tracer studies conducted in July of 1977 were used to probe the transport of airborne pollutants in the land breeze-sea breeze system of the Los Angeles air basin. Sulfur hexafluoride was released from a power plant stack in El Segundo, California. The tracer was carried aloft and out to sea by the nocturnal land breeze. During midmorning the tracer mixed downward to the sea surface and was transported back across the shore during the daytime sea breeze. Further details concerning the tracer transport may be found in Shair, et al. (1981).[3] Our current study seeks to estimate the nominal value and the associated uncertainties in the amount of tracer returned across the shore during the sea breeze.

The total mass balance, for a system without sources, sinks or chemical reaction, may be written as an integral:

$$m_t = \iint_S c' \, \underline{u} \cdot \underline{n} \, dS \, dt \qquad (1)$$

where S is the surface of the control volume, c' is the mass concentration (kg/m^3), $\underline{u}$ is the tracer velocity (m/s), and $\underline{n}$ is a unit normal to the surface, S. In general, c' and $\underline{u}$ are functions of time and position, and the surface any reasonable simply connected region through which all tracer passes. Often the case with field studies, continuous data are not available and the integral is approximated by a discrete summation such as the trapezoidal rule. In this study, the control surface was the coastline between sea level and the mixing height. As indicated in Figure 1, this control surface was represented by 24 line segments. Consequently, equation (1) may be adequately approximated by

$$m_t = \sum_{i=1}^{I} \sum_{j=1}^{J} \sum_{k=1}^{K} \rho \, z_i \, u_{ij} \, c_{ijk} \left[l_{jk}^{(a)} \cos(\theta_{ij} - \phi_{jk}^{(a)}), \right.$$

$$\left. + \, l_{jk}^{(b)} \cos(\theta_{ij} - \phi_{jk}^{(b)}) \right] \Delta t_i \qquad (2)$$

where ρ is the density of pure tracer, z_i is the mixing height, u_{ij} and θ_{ij} are, respectively, the estimated hourly averaged wind speed and direction across each segment, c_{ijk} is the hourly averaged concentration of tracer (assumed to be uniform throughout each segment), and l_{jk} and ϕ_{jk} are the length and normal angle associated with each segment defining the control surface. The time interval, Δt_i, is always one hour, i.e., hourly averaged concentrations were used. Figure 1 shows the locations of wind monitoring stations and air sampling sites. The dotted lines are the coastline segments forming the control surface. Summation is over three subscripts: i, indicates the hour, j, the wind station, and k, the air sampling site. Variables are subscripted as often as the measurements were made. Thus, for example, density was estimated once for the day from the observed average temperature and pressure, while wind velocities were measured every hour and at each of nine stations.

The results of the total mass balance calculations, for both example tests, are shown in Table 1. During both tests, essentially all of the tracer, initially transported out to sea, was returned across the shore on the day of the release. This conclusion agrees with independent calculations reported in Shair et al. (1981).[3] They used another method for constructing the control surface, as well as a different method of wind averaging. The two sets of results differ for this reason, but as will be seen, the discrepancies lie within the calculated uncertainties.

UNCERTAINTY ANALYSIS OF MASS BALANCE

For a function of several variables,

$$y = f(x_1, x_2, \ldots, x_n), \tag{3}$$

the uncertainty in the dependent variable is a function of the uncertainties in each of the independent variables (Bevington, 1969)[4]:

$$\sigma_y^2 = \sum_{i=1}^{n} \sigma_{x_i}^2 \left(\frac{\partial f}{\partial x_i}\right)^2 \tag{4}$$

The partial derivatives are to be evaluated for each variable which is a source of uncertainty. With the assumption that the dependent variables of the mass balance are independent of one another and are evenly and randomly distributed about the actual value of the variable, we may apply the formula to equation (2) for total mass returned to yield

$$\sigma^2_{m_t} = \left[\frac{\sigma_\rho}{\rho}\right]^2 \rho^2 \left(\frac{\partial m_t}{\partial \rho}\right)^2 + \sum_{i=1}^{I} \left(\frac{\sigma_{z_i}}{z_i}\right)^2 z_i^2 \left(\frac{\partial m_t}{\partial z_i}\right)^2$$

$$+ \sum_{i=1}^{I} \sum_{j=1}^{J} \left[\frac{\sigma_{u_{ij}}}{u_{ij}}\right]^2 u_{ij}^2 \left(\frac{\partial m_t}{\partial u_{ij}}\right)^2$$

$$+ \sum_{j=1}^{J} \sum_{k=1}^{K} \left\{ \left[\frac{\sigma_{\ell^{(a)}_{jk}}}{\ell^{(a)}_{jk}}\right]^2 \ell^{2(a)}_{jk} \left(\frac{\partial m_t}{\partial \ell^{(a)}_{jk}}\right)^2 \right.$$

$$\left. + \left[\frac{\sigma_{\ell^{(b)}_{jk}}}{\ell^{(b)}_{jk}}\right]^2 \ell^{2(b)}_{jk} \left(\frac{\partial m_t}{\partial \ell^{(b)}_{jk}}\right)^2 \right\}$$

$$+ \sum_{i=1}^{I} \sum_{j=1}^{J} \sum_{k=1}^{K} \left[\frac{\sigma_{c_{ijk}}}{c_{ijk}}\right]^2 c^2_{ijk} \left(\frac{\partial m_t}{\partial c_{ijk}}\right)^2$$

$$+ \sum_{j=1}^{J} \sum_{k=1}^{K} \left\{ \sigma^2_{\phi^{(a)}_{jk}} \left(\frac{\partial m_t}{\partial \phi^{(a)}_{jk}}\right)^2 + \sigma^2_{\phi^{(b)}_{jk}} \left(\frac{\partial m_t}{\partial \phi^{(b)}_{jk}}\right)^2 \right\}$$

$$+ \sum_{i=1}^{I} \sum_{j=1}^{J} \sigma^2_{\theta_{ij}} \left(\frac{\partial m_t}{\partial \theta_{ij}}\right)^2 \qquad (5)$$

For simplicity and convenience the following assumptions are made about the uncertainties for similar variables

$$\frac{\sigma_{z_1}}{z_1} = \frac{\sigma_{z_2}}{z_2} = \cdots = \frac{\sigma_{z_I}}{z_I} \tag{6}$$

$$\sigma_{\theta_{11}} = \sigma_{\theta_{12}} = \cdots = \sigma_{\theta_{IJ}} \tag{7}$$

etc.

The advantage of these assumptions is that constant factors (here designated by R_α) relate uncertainty in the dependent variables to that in the independent variable. Factoring the like terms outside the various sums results in a compact equation involving each R_α.

$$\sigma_{m_t}^2 = \left[\frac{\sigma_\rho}{\rho}\right]^2 R_\rho + \left[\frac{\sigma_z}{z}\right]^2 R_z + \left[\frac{\sigma_c}{c}\right]^2 R_c + \left[\frac{\sigma_u}{u}\right]^2 R_u$$

$$+ \left[\frac{\sigma_\ell}{\ell}\right]^2 R_\ell + \sigma_\phi^2 R_\phi + \sigma_\theta^2 R_\theta \tag{8}$$

For example, R_z and R_θ are:

$$R_z = \rho^2 \sum_{i=1}^{I} z_i^2 \left\{ \sum_{j=1}^{J} \sum_{k=1}^{K} u_{ij}\, c_{ijk} \left[\ell_{jk}^{(a)} \cos\left(\theta_{ij} - \phi_{jk}^{(a)}\right) + \ell_{jk}^{(b)} \cos\left(\theta_{ij} - \phi_{jk}^{(b)}\right) \right] \right\}^2 \tag{9}$$

$$R_\theta = \rho^2 \sum_{i=1}^{I} \sum_{j=1}^{J} \left[z_i u_{ij} \left(\sin\theta_{ij} \sum_{ij}^{(c)} - \cos\theta_{ij} \sum_{ij}^{(s)} \right) \right]^2 \tag{10}$$

where:

$$\sum_{ij}^{(c)} = \sum_{k=1}^{K} c_{ijk} \left[\ell_{jk}^{(a)} \cos\phi_{jk}^{(a)} + \ell_{jk}^{(b)} \cos\phi_{jk}^{(b)} \right] \tag{11}$$

$$\sum_{ij}^{(s)} = \sum_{k=1}^{K} c_{ijk} \left[\ell_{jk}^{(a)} \sin\phi_{jk}^{(a)} + \ell_{jk}^{(b)} \sin\phi_{jk}^{(b)} \right] \qquad (12)$$

The R factors, which are independent of the uncertainties in the input data, are calculated but once for each test; the uncertainty in the dependent variable is then found from a relatively simple expression. The best estimates for the input variable uncertainties for the two example tests are presented in Table 1, along with the corresponding value of uncertainty in the total mass.

The overall uncertainties, 25% for both tests, reward the effort to include as many data points as possible. Some uncertainty was foreshadowed insofar as the mass balance calculation occasionally showed over a 100% return. In view of the uncertainties there is no catastrophe in finding a nominal value of mass returned slightly above 100%. The interpretation is that essentially all of the tracer passed through the control surface. The calculated uncertainties provide an upper bound as to what constitutes a reasonable and probable total mass return.

The variations in the coefficients of Table 1 merit inspection. As expected from statistics, R_u is smaller than R_ρ because wind speed was measured more frequently than was density. Also, as the number of significant (nontrivial) data points included in the computation increases, the contribution to the uncertainty is softened. Thus, for

example, a very narrow plume would contribute few significant data points and would be characterized by larger R values; uncertainty in the final result would be more sensitive to uncertainties in the input data. For the two example tests, both of which were characterized by broad returning plumes, the R factors were of comparable size. The effect on R values and overall uncertainty due to the number of significant data points contained in a plume will be seen later in the context of Gaussian parameter estimation.

Estimates of the independent variable uncertainties listed in Table 1 came from two sources: observations of random fluctuations due to measurement at a data point, and experiential knowledge of uncertainties brought about by the trapezoidal integral approximations. In particular, uncertainties in wind speed and direction were assigned from average deviations between two adjacent wind stations over a period of time, each assumed to be influenced by the same winds. The contribution to the uncertainty from tracer concentration measurement uncertainty can be estimated from prior experiments. Of less certitude is the accurate assessment of uncertainty contributions brought about by assuming the tracer to be well mixed over the convection layer and over the width of the sampling interval. Knowledge of the plume dispersion history is a guide for estimating such uncertainties.

GAUSSIAN PARAMETER ESTIMATE

Emissions from a point source in a uniform wind field are often distributed downwind in approximate agreement with the Gaussian model, in which the height and width of the concentration profile are correlated with atmospherice stability (Turner, 1970).[5] Under such conditions the tracer data can easily be reduced and the results compared to the predictions of the Gaussian model with the aid of integral identities for the plume parameters. The Gaussian parameters to be estimated are the horizontal standard deviation in concentration, σ_{hd}, the plume centerline, y_o, and the centerline concentration, c_{max}. From these parameters it is possible to estimate either the vertical standard deviation in concentration, σ_{vd}, (or, alternately, the well mixed depth of the tracer plume), or, if the vertical distribution is also measured, a mass flux balance (a comparison between observed and released tracer fluxes).

The horizontal distribution of tracer for a Gaussian plume may be described by

$$c(y) = c_{max}\, e^{-\frac{(y-y_o)^2}{2\sigma_{hd}^2}} \qquad (13)$$

where the parameters are the same as those defined above. By standard statistical techniques, the Gaussian plume parameters can be determined from the zeroeth, first, and second moment integrals of the continuous concentration distribution,

$$I_0 = \int_{-\infty}^{\infty} c(y)\, dy \tag{14}$$

$$I_1 = \int_{-\infty}^{\infty} yc(y)\, dy \tag{15}$$

$$I_2 = \int_{-\infty}^{\infty} y^2 c(y)\, dy \tag{16}$$

The appropriate formulae for the plume centerline location, crosswind standard deviation in concentration, and the centerline maximum concentrations are:

$$y_0 = I_1/I_0 \tag{17}$$

$$\sigma_{hd}^2 = I_2/I_0 - y_0^2 \tag{18}$$

$$c_{max} = I_0/\sqrt{2\pi}\sigma_{hd} \tag{19}$$

For sampling traverses which are not straight, or oriented precisely crosswind, suitable average correction factors can be applied, or the traverse data projected, point by point, onto a straight line segment which is orthogonal to the wind. In order to limit the influence of low concentrations far from the plume centerline, where, presumably, the tracer detection technique is less accurate, the integration interval is contracted, excluding concentrations less than 10% of the maximum. The neglected integral area can be included by applying a correction factor for neglected area under a suitably normalized exact Gaussian curve. The normalization procedure includes choosing an exact Gaussian distribution with the same centerline maximum concentration and standard deviation in concentration, σ_{hd}, and by shifting the abscissa of the experimental data to align the origin with the plume centerline. This normalization procedure gives the following relations between the complete (I) and contracted integrals (I'):

$$I_0 = k_0 I_0' \tag{20}$$

$$I_1 = k_1 I_1' \tag{21}$$

$$I_2 = k_2 I_2' \tag{22}$$

where

$$k_0 = 1.032925 \tag{23}$$

$$k_1 = 1.032925 \tag{24}$$

$$k_2 = 1.254861 \tag{25}$$

The algorithm used here for estimating the appropriate Gaussian parameters is:

(1) Evaluate plume centerline location using all data, including data points extending past concentrations less than 10% of the observed maximum.

(2) Shift the position coordinate axis so that the plume centerline, calculated above, coincides with the origin.

(3) Evaluate the horizontal dispersion coefficient, σ_y, and the plume centerline concentration, c_{max}, using the fully extended limits of integration as in step 1.

(4) By interpolating (linearly or otherwise) between appropriate points, find the location corresponding to 10% of the centerline concentration as calculated in step 3.

(5) Recalculate the best fit Gaussian parameters by evaluating the appropriate integrals between the limits specified in step 4.

(6) If necessary, repeat steps 4 and 5 until the limits of integration are at 10% of the recalculated maximum concentration.

Additionally, as was done for the total mass balance, the trapezoidal rule is used to approximate the integrals to accommodate discrete sampling. For four data points equidistant in the integration interval (interval defined as the region between the locations corresponding to 10% of the maximum concentration), the errors introduced by the trapezoidal approximation are no more than 4%: plume centerline location calculations are affected least by the approximation. Fewer data points lead to significantly larger errors in the parameter estimation. A rule of thumb is, therefore, to have at least one data point every horizontal standard deviation, σ_y, across the plume, since the 10% limits encompass about a 4.3 σ_y distance in the plume.

Two SF_6 releases in the Santa Barbara Channel conducted on September 24 and 28, 1980, under stable transport conditions gave rise to concentration profiles suitable for comparison to the

Gaussian model (Reible, 1981)[6]. The tracer was released from 9 km offshore, as indicated in Figure 1. Grab samples were gathered by automobile teams traversing along the coastline between hourly-averaged sampling locations 1 and 2 in Figure 1. The observed concentration profiles are indicated in Figure 2. Using the formulae developed above for finding Gaussian plume parameters, concentration versus distance data for the three traverses were reduced; the results are contained in Table 2. In all instances the calculated horizontal dispersion parameter indicated greater stability than might be anticipated from the vertical temperature profile. It should be noted, however, that the automobile traverse data represent short time averages (between 3 and 10 minutes). As the sample averaging time increases, the observed plume generally becomes flatter and broader due to meandering of the wind (Reible, 1981)[6]. This could account for the difference between the observed atmospheric stability and that indicated by the tracer data.

UNCERTAINTY ANALYSIS OF GAUSSIAN PARAMETER ESTIMATES

Analogous to the procedure used for the total mass balance calculation, equation (4) may be applied to the formulae for the Gaussian plume parameters. We collect terms assuming the same uncertainty in similar variable, i.e., assuming

$$\sigma_{y_1} = \sigma_{y_2} = \cdots = \sigma_{y_n} \tag{26}$$

$$\frac{\sigma_{c_1}}{c_1} = \frac{\sigma_{c_2}}{c_2} = \cdots = \frac{\sigma_{c_n}}{c_n} \tag{27}$$

we obtain

$$\sigma_{y_0} = \sigma_y^2 R_y^{(y_0)} + \left[\frac{\sigma_c}{c}\right]^2 R_c^{(y_0)} \tag{28}$$

$$\sigma_{\sigma_{hd}} = \sigma_y^2 R_y^{(\sigma_y)} + \left[\frac{\sigma_c}{c}\right]^2 R_c^{(\sigma_y)} \tag{29}$$

$$\sigma_{c_{max}} = \sigma_y^2 R_y^{(c_{max})} + \left[\frac{\sigma_c}{c}\right]^2 R_c^{(c_{max})} \tag{30}$$

Equations 28-30 simply describe the dependence of the uncertainty in the various plume parameters upon uncertainty in position and uncertainty in concentration. Estimates for the uncertainty in postion and concentration, the R factors for equations 28-30, and the final results of the calculations are shown in Table 2. Note the

lesser uncertainty for Test 1, with its wider plume: more significant data points are included in the determination of the Gaussian parameters.

Distinct from the issue of input data uncertainty is whether a Gaussian model accurately depicts the physical situation. Using a standard statistical technique, the so-called chi-squared test, the deviations of the experimental data from the fitted Gaussian curves indicate that the parent distribution of tracer is not Gaussian (Bevington, 1969).[4] Due to nonuniformities in the mean and turbulent wind field, the assumption that the tracer is normally distributed crosswind is but a crude approximation. It is, however, a level of approximation consistent with the current state of knowledge on dispersion in the atmosphere, and, for plumes such as those of Figure 2, a very useful approximation.

SUMMARY AND CONCLUSIONS

A method for estimating nominal values and uncertainties associated with mass balances has been demonstrated by way of example. For the cases studied the nominal values of mass returned across the shore were in good agreement with that known to have been released into the land breeze; that is, essentially all of the tracer returned across the control surface. In these cases the total uncertainties in the nominal values (about 25%) were actually less than the uncertainty in any individual measurement of concentration or mixing height (30%-40%). This is simply a reflection of the effect of statistical cancellation of errors distributed randomly about the actual value of the measured variables, but, nonetheless, clearly demonstrates that a complicated calculation such as the tracer mass balance may be subject to less uncertainty than might otherwise be expected.

A technique for fitting data to the Gaussian plume model was also demonstrated, using the integral definitions of the Gaussian dispersion parameters. The technique presented was relatively insensitive to uncertainties in the data; relative uncertainty in plume centerline location and horizontal standard deviation in concentration were much less than the relative uncertainties in individual measurements of concentration or location. However, to ensure good results at least four approximately equidistant sampling points must lie between the locations corresponding to 10% of the

maximum concentration, i.e., data points should be spaced no farther than one σ_y apart.

Acknowledgments

The authors wish to thank Professor Gary Lorden of Caltech, and Charles Bennett of the California Air Resources Board for their interesting and helpful discussions. This work was supported partly by the California Air Resources Board, and partly by the Caltech Environmental Quality Laboratory through a grant from the Andrew W. Mellon Foundation.

References

1 Lamb, B. K., "Development and Application of Dual Atmospheric Tracer Techniques for the Characterization of Pollutant Transport and Dispersion," Ph.D. Thesis, California Institute of Technology, Pasadena, CA, 1978.

2 Reible, D. D., "An investigation of the Transport and Dispersion of Atmospheric Contaminants in the Mountain-Valley and Coastal Regions of California," Ph.D. Thesis, California Institute of Technology, Pasadena, CA, 1982.

3 Shair, F. H., Sasaki, E. J., Carlan, D. E., Cass, G. R. Goodin, W. R., Edinger, J. G., and Schacher, G. E., "Transport and Dispersion of Airborne Pollutants Associated with the Land Breeze-Sea Breeze System," Atmospheric Environment, (1981).

4 Bevington, P. R., Data Reduction and Error Analysis for the Physical Sciences, McGraw-Hill, New York, pp. 56-60, 1969.

5 Turner, B., "Workbook of Atmospheric Dispersion Estimates," U.S. Environmental Protection Agency, Research Triangle Park, North Carolina, 1970.

6 Reible, D. D., and Shair, F. H., "The Transport and Dispersion of Airborne Contaminants in the Santa Barbara Channel Area of Southern California," submitted to Atmospeheric Environment.

Table 1

Total Mass Balance and Uncertainty Analysis

Test Number	1	2
Date of Test	July 22, 1977	July 24, 1977
Amount SF_6 released (grams)	90,800	236,080
Amount SF_6 returned (grams)[a]	111,244	211,917
Percentage return[a]	123	90
Amount SF_6 returned (grams)[b]	95,490	244,569
Percentage return[b]	105	104
R-factors:		
R_ρ	1.000	1.000
R_z	0.165	0.165
R_c	0.038	0.034
R_u	0.067	0.080
R_ℓ	0.082	0.052
R_ϕ	0.013	0.026
R_θ	0.055	0.062
Estimated uncertainty in raw data:		
ρ - density (%)	5	
z - inversion height (%)	40	
c - SF_6 concentration (%)	30	
u - wind speed (%)	25	
ℓ - coastal length (%)	10	
ϕ - coastal angle (radians)	0.175	
θ - wind direction (radians)	0.698	
Calculated uncertainty in		
m_t - total mass returned (%)	25.4	25.5

[a](This calculation)

[b](Calculation of Shair, et al., 1981)

Table 2

Gaussian Plume Parameters and Uncertainty Analysis

Traverse number	1	2*	3*
Date of test	9/24/80	9/28/80	9/28/80
Plume parameters			
y_o (km)	3.38	1.56	1.54
σ_{hd} (km)	0.38	0.23	0.18
c_{max} (ppt)	2730	9150	9410
R-factors:			
$R_c^{(y_o)}$	0.0033	0.0027	0.0013
$R_c^{(\sigma_y)}$	0.032	0.040	0.052
$R_c^{(c_{max})}$	0.25	0.40	0.51
$R_y^{(y_o)}$	0.05	0.10	0.06
$R_y^{(\sigma_y)}$	0.040	1.14	0.60
$R_y^{(c_{max})}$	0.92	2.92	1.99
Estimated uncertainty in raw data:			
σ_c - concentration (%)		30	
σ_y - distance crosswind (km)		0.16	
Calculated uncertainty in			
y_o (km)	0.06	0.08	0.06
σ_y (%)	11.5	18.2	14.2
c_{max} (%)	21.5	33.4	31.2

*These traverses were within one hour of one another, during the same release.

Title of Figures

Figure 1 - Locations of hourly average sampling sites (only 24 of 29 were used in each test), wind monitoring stations, and the release point for the tests of the mass balance calculation. Also included is the location of the release location for the tests used in the Gaussian parameter estimation.

Figure 2 - Concentration profiles from automobile traverses. Gaussians are fit to three traverses; the last two traverses were of the sampe plume and the fitted curve combines both data sets. The shaded region indicates the limits of the integration for the curve fitting procedure.

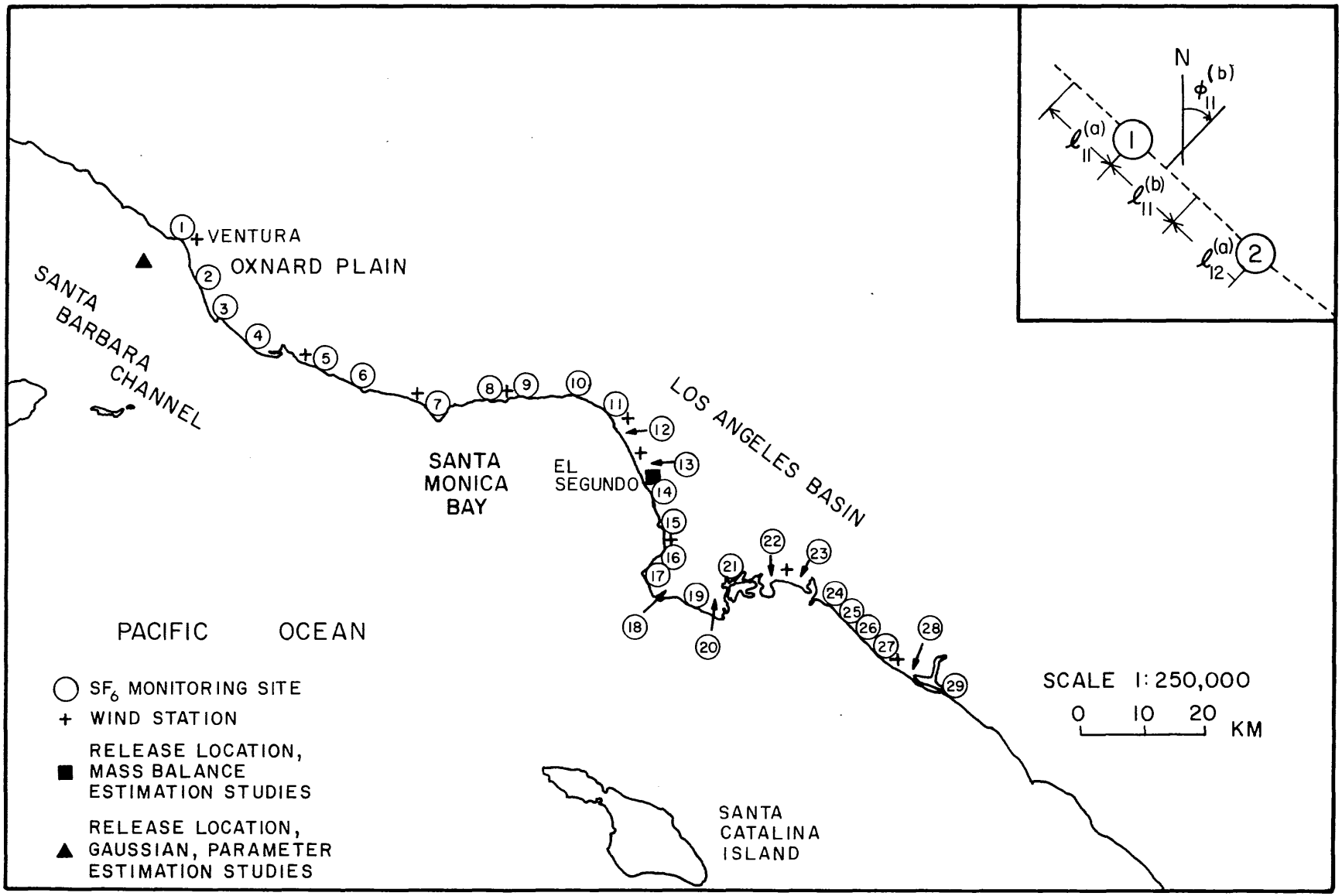
N
$\phi_{11}^{(b)}$
$\ell_{11}^{(a)}$
1
$\ell_{11}^{(b)}$
$\ell_{12}^{(a)}$
2
VENTURA
OXNARD PLAIN
SANTA BARBARA CHANNEL
SANTA MONICA BAY
EL SEGUNDO
LOS ANGELES BASIN
PACIFIC OCEAN
SANTA CATALINA ISLAND
SCALE 1:250,000
0 10 20 KM
SF6 MONITORING SITE
WIND STATION
RELEASE LOCATION, MASS BALANCE ESTIMATION STUDIES
RELEASE LOCATION, GAUSSIAN, PARAMETER ESTIMATION STUDIES

Figure 1

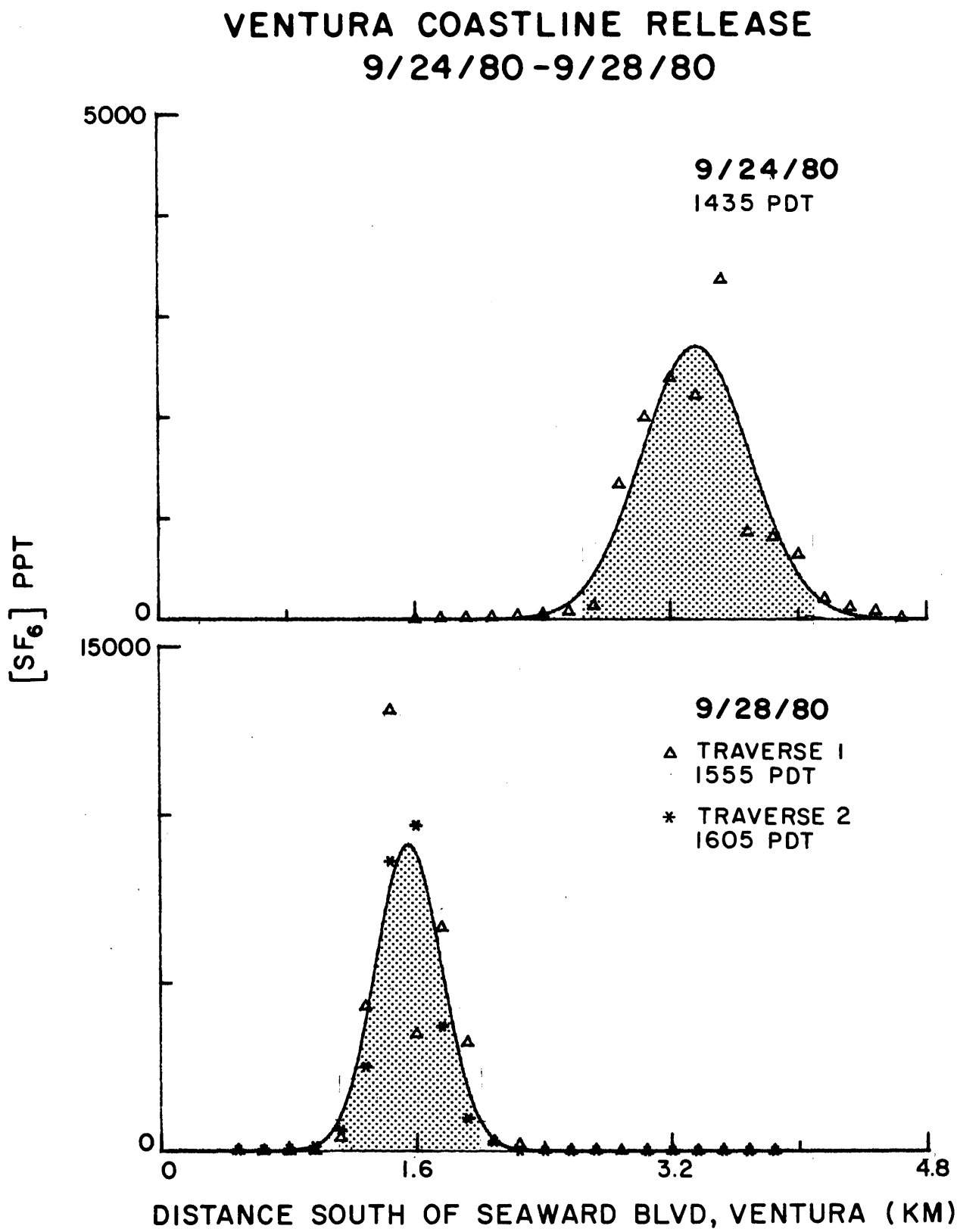
VENTURA COASTLINE RELEASE
9/24/80-9/28/80
5000
0
9/24/80
1435 PDT
15000
0
9/28/80
TRAVERSE 1
1555 PDT
TRAVERSE 2
1605 PDT
[SF6] PPT
0
1.6
3.2
4.8
DISTANCE SOUTH OF SEAWARD BLVD, VENTURA (KM)

Figure 2

Chapter 6

Sulfate Data at Lennox, Redondo Beach, and Santa Catalina Island in July 1977

George Tsou
Dennis Gibbons
D. William Davis
Shake' Sarkissian

October, 1977

Aerosol Laboratory
Atmospheric Studies
Haagen Smit Laboratory
Air Resources Board
9528 Telstar Ave.
El Monte, CA 91731

Introduction:

The aerosol studies section of the Research Division ARB participated in the ARB-Cal Tech Acania project conducted during July 1977. Low-volume sequential samplers were located at Redondo Beach, Lennox, and Santa Catalina Island. The Redondo Beach sampler was located on the roof of the Fire Department. The Lennox sampler was located on the roof of the SCAQMD station. The Santa Catalina sampler was located on the roof of the USC-Marine Science Center near Two Harbors.

Two-hour samples were collected at 4-5 cfm 24 hours a day. The 47 mm Gelman GA-1 filters were analyzed for sulfate by our X-ray Fluorescence technique.

Herein we report the sulfate data.

Le x

Sulfate in $\mu g/m^3$

Date \ Time (PDT	00	02	04	06	08	10	12	14	16	18	20	22
July 18, 1977							10.6	12.8	14.2	11.4	11.4	9.9
July 19, 1977	11.9	9.8	10.5	16.8	20.0	14.7	*	*	*	*	*	*
July 20, 1977	*	*	*	*	*	*	13.2	14.3	19.7	27.5	25.0	28.0
July 21, 1977	29.8	43.7	39.1	33.3	34.6	48.0	41.9	37.9	30.6	16.1	14.1	15.5
July 22, 1977	20.2	28.3	34.5	34.0	41.8	58.0	49.9	41.0	26.6	20.6	14.1	19.2
July 23, 1977	30.8	33.9	43.0	42.6	44.8	30.7	16.6	21.2	16.0	18.6	18.2	19.6
July 24, 1977	*	*	23.0	24.2	*	*	32.2	30.1	22.1	17.4	10.8	8.5
July 25, 1977	6.9	8.0	8.3	10.0	12.8	16.7	4.0	10.7	12.3	11.3	9.8	7.1
July 26, 1977	7.1	6.0	6.6	9.1	12.6	*	20.4	11.2	9.2	11.8	7.7	5.5
July 27, 1977	7.0	7.9	8.4	12.8	15.0	25.3	17.5	17.4	15.2	*	7.8	*

* voided data

L ox

Sulfate in $\mu g/m^3$

Time (PDT / Date	00	02	04	06	08	10	12	14	16	18	20	22
July 28, 1977	*	23.5	17.7	16.3	*	17.9	30.4	32.8	29.0	29.0	30.3	26.5
July 29, 1977	24.3	21.9	26.2	30.2	28.8							
July 30, 1977												

Summer Sulfate Program

Redondo Beach

Sulfate in $\mu g/m^3$

Date \ Time (PDT	00	02	04	06	08	10	12	14	16	18	20	22
July 18, 1977	6.1	4.6	5.4	6.4	7.2	5.0	4.6	4.1	9.4	7.9	5.2	7.1
July 19, 1977	6.4	8.4	9.0	12.6	13.1	7.3	5.5	6.3	6.8	9.2	19.6	23.7
July 20, 1977	23.3	21.1	16.3	13.3	11.4	7.7	7.1	8.5	12.2	16.3	16.7	25.8
July 21, 1977	21.4	22.8	30.6	31.5	36.7	43.3	38.2	37.9	26.4	17.4	13.9	9.4
July 22, 1977	24.5	29.9	33.5	40.1	50.2	44.5	36.6	25.3	12.6	11.1	11.5	18.1
July 23, 1977	24.9	25.7	29.3	30.5	35.4	25.0	17.9	10.0	9.4	9.3	10.6	18.4
July 24, 1977	16.8	17.4	19.5	20.1	22.7	25.2	27.0	19.4	18.3	5.9	4.1	5.5
July 25, 1977	3.9	4.3	5.3	8.2	5.5	*	5.9	4.8	5.3	5.7	5.0	5.8
July 26, 1977	5.7	6.9	7.7	7.7	6.0	9.2	6.9	5.6	4.7	5.2	4.5	4.8
July 27, 1977	7.6	8.8	6.1	8.4	6.5	5.0	5.5	6.6	4.7	3.5	5.4	3.3

Redondo Beach

Sulfate in $\mu g/m^3$

Date \ Time (PDT	00	02	04	06	08	10	12	14	16	18	20	22
July 28, 1977	12.5	14.5	16.5	18.3	16.5	21.0	26.2	26.9	23.5	24.2	25.8	17.7
July 29, 1977	18.2	20.5	21.2	30.3	30.1	19.4	13.8	6.0	5.2	5.5	3.8	4.7
July 30, 1977	7.6	7.6	10.3	16.6	20.2							

Summer Program

Santa Catalina

Sulfate in $\mu g/m^3$

Date \ Time (PDT	00	02	04	06	08	10	12	14	16	18	20	22
July 12, 1977	9.2	13.0	15.4	16.2	9.1	6.4	10.2	9.1	4.4	2.9	2.4	2.6
July 13, 1977	3.7	4.3	6.8	7.1	6.0	6.1	3.0	4.7	3.6	3.4	3.4	4.1
July 14, 1977	6.2	8.6	10.0	10.4	11.6	9.4	8.6	6.6	7.5	11.1	7.5	5.9
July 15, 1977	6.7	8.4	7.8	11.4	11.4	10.3	10.0	9.2	8.6	8.4	7.6	6.2
July 16, 1977	5.0	5.2	5.5	5.4	5.1	9.8	13.2	9.5	7.0	6.8	9.8	11.6
July 17, 1977	9.2	6.1	5.4	6.4	5.0	5.8	6.8	4.3	3.1	4.7	3.8	4.0
July 18, 1977	4.0	4.2	5.6	4.8	3.6	3.8	4.2	7.3	4.3	3.0	2.6	3.2
July 19, 1977	4.6	5.4	5.2	5.6	7.1	7.6	6.1	4.9	5.2	5.1	5.1	7.0
July 20, 1977	6.8	7.3	8.3	8.6	7.8	*	10.0	10.3	9.8	8.4	9.3	9.8
July 21, 1977	12.6	11.0	10.5	12.2	12.3	*	11.4	15.9	18.3	11.9	7.2	10.7

* Voided data

SUMMER . OGRAM

Santa Catalina

Sulfate in $\mu g/m^3$

Time (PDT / Date	00	02	04	06	08	10	12	14	16	18	20	22
July 22, 1977	6.9	5.2	4.0	9.2	12.1	13.0	10.8	12.2	11.3	10.0	6.4	9.6
July 23, 1977	11.2	13.1	14.0	11.9	11.0	11.9	10.8	11.7	8.7	8.7	13.1	13.8
July 24, 1977	12.0	12.5	12.2	13.6	11.1	9.0	27.4	22.0	19.3	15.7	5.2	6.6
July 25, 1977	3.8	4.1	7.7	9.0	13.1	12.0	8.2	5.8	5.0	4.7	4.0	4.3
July 26, 1977	4.8	3.7	3.6	3.7	3.8	3.8	5.2	5.8	4.1	4.9	3.7	2.2
July 27, 1977	2.7	2.3	2.5	2.9	3.3	1.8	4.4	6.3	7.0	5.6	4.6	3.5
July 28, 1977	3.7	3.8	3.2	3.7	5.9	5.6	3.8	4.4	4.9	9.5	16.9	14.1
July 29, 1977	12.2	9.6	8.4	6.5	5.5	5.9	4.0	4.2	3.5	5.2	4.5	4.8
July 30, 1977	4.5	5.5	5.8	7.0	6.9							

[illegible] Station: Santa Catalina - Two Harbors

Reporting Agency: [illegible] - Atmospheric Studies

Read by: [illegible] & CR Checked by: JS Date 3-11-77

SO_2 (Parts Per [illegible])

DAY	00	01	02	03	04	05	06	07	08	09	10	11	12	13	14	15	16	17	18	19	20	21	22	23	DAILY PEAK Conc	DAILY PEAK Time
1																										
2																										
3																										
4																										
5																										
6																										
7																										
8																										
9																										
10																										
11																										
12			[illegible]																							
13	5.0	[illegible]	5.0	5.0	5.0	5.0	5.0	5.0	5.0	5.0	5.0	5.0	5.0	5.0	5.0	5.0	5.0	5.0	5.0	5.0	5.0	5.0	5.0	5.0	—	—
14	5.0	5.0	5.0	5.0	5.0	5.0	5.0	5.0	5.0	5.0	5.0	5.0	5.0	5.0	5.0	5.0	5.0	5.0	5.0	5.0	5.0	5.0	5.0	5.0	—	—
15	5.0	5.0	5.0	5.0	5.0	5.0	5.0	5.0	5.0	5.0	5.0	6.0	5.0	6.0	7.0	8.0	7.0	6.0	5.0	5.0	5.0	5.0	6.0	5.0	9.0	1500
16	2.0	2.0	2.0	2.0	2.0	2.0	2.0	2.0	2.0	2.0	2.0	2.0	NR	3.0	3.0	2.0	2.0	2.0	2.0	2.0	2.0	2.0	3.0	2.0	5.0	1320
17	2.0	2.0	3.0	2.0	2.0	3.0	3.0	4.0	NR	2.0	2.0	2.0	2.0	2.0	2.0	2.0	2.0	2.0	2.0	2.0	2.0	3.0	2.0	2.0	5.0	0215
18	2.0	2.0	2.0	2.0	2.0	2.0	2.0	2.0	2.0	2.0	2.0	2.0	2.0	2.0	2.0	2.0	2.0	2.0	2.0	2.0	2.0	3.0	2.0	2.0	4.0	2115
19	2.0	2.0	2.0	2.0	2.0	2.0	3.0	3.0	4.0	NR	5.0	6.0	6.0	5.0	5.0	5.0	5.0	4.0	4.0	3.0	3.0	4.0	4.0	3.0	10.0	1600
20	3.0	4.0	4.0	4.0	4.0	4.0	4.0	NR	2.0	2.0	2.0	2.0	3.0	3.0	3.0	3.0	4.0	3.0	3.0	4.0	4.0	5.0	5.0	6.0	11.0	0525
21	5.0	5.0	5.0	5.0	5.0	5.0	6.0	7.0	7.0	6.0	6.0	6.0	5.0	6.0	5.0	4.0	4.0	3.0	4.0	5.0	5.0	5.0	5.0	6.0	9.0	0310430
22	5.0	5.0	5.0	5.0	5.0	5.0	6.0	5.0	5.0	5.0	4.0	4.0	4.0	4.0	4.0	4.0	4.0	4.0	4.0	4.0	4.0	5.0	6.0	4.0	10.0	2110
23	7.0	7.0	7.0	8.0	7.0	8.0	7.0	6.0	6.0	3.0	2.0	1.0	2.0	2.0	2.0	2.0	3.0	3.0	3.0	3.0	5.0	4.0	3.0	3.0	11.0	0800
24	3.0	3.0	3.0	4.0	5.0	5.0	5.0	4.0	3.0	5.0	5.0	8.0	6.0	5.0	5.0	5.0	5.0	5.0	5.0	6.0	5.0	7.0	6.0	6.0	14.0	1150
25	7.0	7.0	7.0	7.0	7.0	8.0	8.0	5.0	6.0	6.0	6.0	6.0	6.0	5.0	4.0	3.0	2.0	3.0	2.0	3.0	2.0	2.0	2.0	3.0	12.0	1300
26	1.0	1.0	1.0	2.0	2.0	2.0	2.0	2.0	3.0	5.0	5.0	5.0	8.0	8.0	8.0	7.0	3.0	4.0	5.0	5.0	5.0	5.0	5.0	5.0	9.0	1320
27	3.0	2.0	2.0	2.0	3.0	5.0	4.0	5.0	5.0	4.0	4.0	4.0	5.0	4.0	5.0	4.0	4.0	5.0	5.0	5.0	5.0	5.0	5.0	5.0	9.0	1630
28	4.0	3.0	3.0	3.0	3.0	4.0	4.0	4.0	3.0	2.0	1.0	<1.0	<1.0	<1.0	<1.0	<1.0	<1.0	4.0	4.0	<1.0	<1.0	<1.0	<1.0	<1.0	6.0	0615
29	1.0	2.0	2.0	2.0	2.0	2.0	2.0	3.0	3.0	4.0	2.0	2.0	2.0	2	[illegible]	2.0	2.0	2.0	2.0	2.0	2.0	3.0	2.0	2.0	6.0	0920
30	2.0	[illegible]	2.0	7.0	3.0	3.0	4.0	4.0	← END																	